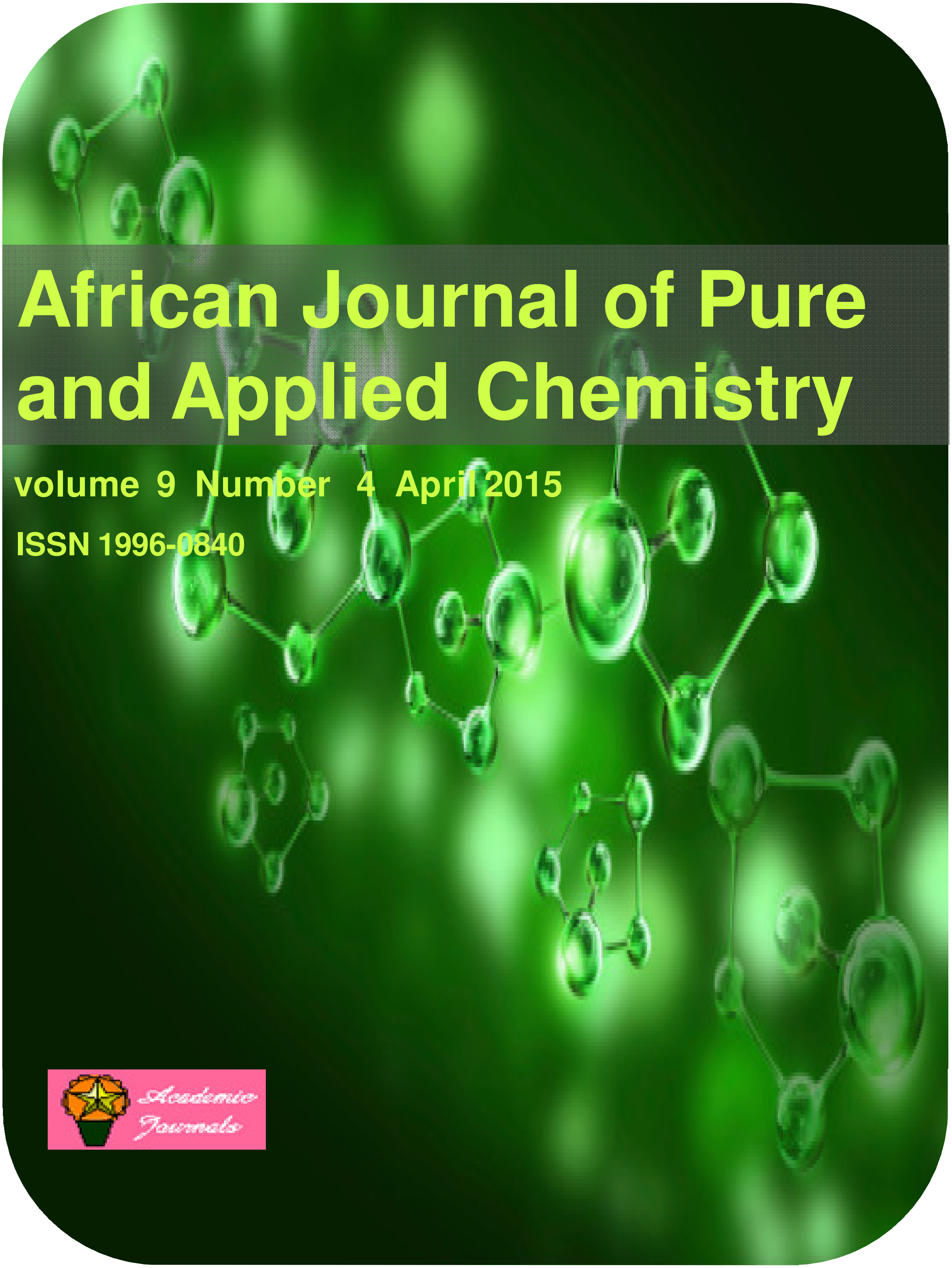

African Journal of Pure and Applied Chemistry

volume 9 Number 4 April 2015

ISSN 1996-0840

Academic Journals

ABOUT AJPAC

The **African Journal of Pure and Applied Chemistry (AJPAC)** is an open access journal that publishes research analysis and inquiry into issues of importance to the science community. Articles in AJPAC examine emerging trends and concerns in the areas of theoretical chemistry (quantum chemistry), supramolecular and macromolecular chemistry, relationships between chemistry and environment, and chemicals and medicine, organometallic compounds and complexes, chemical synthesis and properties, chemicals and biological matters, polymer synthesis and properties, nanomaterials and nanosystems, electrochemistry and biosensors, chemistry and industry, chemistry and biomaterials, advances in chemical analysis, instrumentation, speciation, bioavailability. The goal of AJPAC is to broaden the knowledge of scientists and academicians by promoting free access and provide valuable insight to chemistry-related information, research and ideas. AJPAC is a bimonthly publication and all articles are peer-reviewed.

African Journal of Pure and Applied Chemistry (AJPAC) is published twice a month (one volume per year) by Academic Journals.

Contact Us

Editorial Office: ajpac@academicjournals.org

Help Desk: helpdesk@academicjournals.org

Website: http://www.academicjournals.org/journal/AJPAC

Submit manuscript online http://ms.academicjournals.me/.

Editors

Editorial Board

Dr. Fatima Ahmed Al-Qadri
Asst. Professor
Chemistry Department
Sana'a University
Republic of Yemen.

Dr. Aida El-Azzouny
National Research Center
(NRC, Pharmaceutical and
Drug Industries Research Division)
Dokki-Cairo, 12622-Egypt.

Dr. Santosh Bahadur Singh
Department of Chemistry
University of Allahabad
Allahabad, India.

Dr. Gökhan Gece
Department of Chemistry
Bursa Technical University
Bursa, Turkey.

Dr. Francisco Torrens
Institute for Molecular Science
University of Valencia
Paterna Building Institutes
P. O. Box 22085
E-46071 Valencia
Spain.

Dr. Erum Shoeb
Asst. Professor
Department of Genetics
University of Karachi
Karachi-75270
Pakistan.

Dr. Ishaat Mohammad Khan
Physical Research Laboratory
Department of Chemistry
Aligarh Muslim University
Aligarh 202002, India.

Prof. Jean-Claude Bunzli
Department of Chemistry
Swiss Federal Institute of Technology Lausanne
(EPFL)
Institute of Chemical Sciences and Engineering
BCH 1402
CH-1015 Lausanne (Switzerland).

Mrinmoy Chakrabarti
Department of Chemistry,
Texas A&M University
415 Nagle Street, College Station, TX 77840
USA.

Dr. Geoffrey Akien
430 Eisenhower Drive, Apartment B-2,
Lawrence, Kansas 66049,
United States.

Prof. Anil Srivastava
Jubilant Chemsys Ltd.,
B-34, Sector-58,
Noida 201301 (UP),
India.

African Journal of Pure and Applied Chemistry

Table of Contents: Volume 9 Number 4 April, 2015

ARTICLES

Research Articles

Estimation of the refractive indices of some binary mixtures
Isehunwa S. O., Olanisebe E. B., Ajiboye O. O. and Akintola S. A. **58**

Oxidation of acha (Digitaria exilis) starch using 3.5% active chlorine sodium hypochlorite
S. Isah, A. A. Oshodi and V. N. Atasie **65**

Reversal of plasticity of acid leached kaolinitic clays from Mukurwe-ini
Dickson Andala and Wachira David Maina **71**

academicJournals

Vol. 9(4), pp. 58-64, April, 2015
DOI: 10.5897/AJPAC2015.0613
Article Number: 28B614952528
ISSN 1996 - 0840

http://www.academicjournals.org/AJPAC

African Journal of Pure and Applied Chemistry

Full Length Research Paper

Estimation of the refractive indices of some binary mixtures

Isehunwa S. O.*, Olanisebe E. B., Ajiboye O. O. and Akintola S. A.

Department of Petroleum Engineering, University of Ibadan, Nigeria.

Received 4 February, 2015; Accepted 5 March, 2015

Refractive index is a useful fluid characterization parameter with widespread industrial applications. The values for many pure liquids are known or readily available in literature. However, when experimental data are not available, the refractive indices of binary and multi-component liquids are often estimated from the pure components using mixing rules which are sometimes not accurate. This study was designed to measure the refractive indices and evaluate the accuracy of some commonly used mixing rules when applied to benzene-toluene, heptane-hexane, hexane-acetone, heptane-acetic acid and acetic acid-acetone binary mixtures at varying volume fractions and temperatures between 20 and 60°C. A simpler relation based on modified Kay or Arago-Biot mixing rule was demonstrated to have wider range of applicability because of the explicit temperature-dependence term.

Key words: Refractive index, mixing rule, binary mixtures, excess volume, refractometer.

INTRODUCTION

Refractive index is a fundamental physical property which measures the speed of light in a material and characterizes its optical properties (Singh, 2002). It has been used for many years for accurate identification and characterization of pure fluids and mixtures (Ebatco, 2013). Sharma et al. (2007) and Vural et al. (2011) noted that refractive index, density and viscosity are essential for the characterisation and understanding of the thermodynamic properties of fluids. The molecular interaction in a fluid mixture can also be assessed from the refractive index and density of its pure components (Leron et al., 2012; Rilo et al., 2012).

Refractive index is useful in the indirect measurement of density and salinity and in the detection of structural properties of liquid-liquid mixtures. Its application has also led to the development of alternatives in fuel substitutes, additives, and treatment of oils with chemicals (Rushton, 1955). Wankhede (2011) used mixing rule to determine the composition of an unknown mixture and the presence of molecular interactions in binary mixtures. Several researchers have noted that deviation between theoretical and experimental values of the refractive indices of mixtures can be reduced by considering the concept of excess volume (Mehra, 2003; Ali and Tariq 2006, Sharma et al., 2007; Meenachi and Krishnamurthi, 2013).

The refractive indices of pure, binary and multi-component fluids can readily be measured directly using refractometers. However, there are times when the experimental values are not available and it is desirable to estimate the refractive index of binary or multi-component liquids from the pure components by using

---

*Corresponding author. E-mail: Sunday.isehunwa@gmail.com

mixing rules. The most commonly used mixing rules are the Lorentz-Lorenz equation, Weiner relation, Heller's and Gladstone-Dale equations. These mixing rules apply the concept of excess molar properties, a measure of thermodynamic interaction changes with physical forces in polar molecules (Vural et al., 2011). They therefore require rigorous procedures.

The aim of this study was to develop an accurate mixing rule that is simpler to apply than the commonly used relations. The refractive indices of pure components and mixtures were measured at different temperatures and volume fractions and the results were used to develop a simple equation based on the modification of the Kay or Arago-Biot mixing rule. The resultant temperature-dependent relation proved accurate and easy to use.

Theoretical basis

In the process of mixing two or more components effects such as the structural re-orientation occurs due to the differences in shape and size of component molecules and the interaction between molecules (Ali et al., 2008). If we assume that volumes of the pure components can be added when analyzing fluid mixtures (Andrew et al., 1986) and using the mean polarizability which approximates the average possible orientations of a molecule, the Lorentz-Lorenz (1979) relation can be obtained which for a binary mixture is expressed as:

$$\frac{n_m^2 - 1}{n_m^2 + 2} = y_1 \frac{n_1^2 - 1}{n_1^2 + 2} + y_2 \frac{n_2^2 - 1}{n_2^2 + 2} \qquad (1)$$

The Weiner relation is given as:

$$\frac{n_m^2 - n_1^2}{n_m^2 + 2n_1^2} = y_2 \frac{n_2^2 - n_1^2}{n_2^2 + 2n_1^2} \qquad (2)$$

While Heller relation is:

$$\frac{n_m - n_1}{n_1} = \frac{3}{2} y_2 \frac{m^2 - 1}{m^2 + 2} \qquad (3)$$

Where, $m = n_2/n_1$

And, the Gladstone-Dale equation can be expressed as:

$$\frac{n_m - 1}{\rho_m} = \left(\frac{n_1 - 1}{\rho_1}\right) w_1 + \left(\frac{n_2 - 1}{\rho_2}\right) w_2 \qquad (4)$$

Where: $n_m = refractive\ index\ of\ mixture$,

$n_1, n_2 = Refractive\ index\ of\ pure\ components,$

$y_1\ and\ y_2 = volume\ fractions$,

$w_1\ and\ w_2 = weight\ fractions$,

$\rho_m = density\ of\ mixture$,

If we assume that there is volume additivity during mixing, we can use the simple Arago-Biot relation:

$$n_m = n_1 y_1 + n_2 y_2 \qquad (5)$$

However, for most fluid mixtures, $\sum_i y_i \neq 1$ since there is volume change during mixing (Brocos et al, 2003). Therefore, adapting the method of Leron et al (2012), we propose a modified Arago-Biot equation as:

$$n_m = (y_1 n_1 + m_{d1}) + (y_2 n_2 + m_{d2}) \qquad (6)$$

Where,

$$m_{di} = \frac{y_i (\sqrt{n_m})}{1000} \qquad (7)$$

i= 1, 2

$and\ m_{di}\ and\ m_{dj} = 0\ \ for\ pure\ components$

MATERIALS AND METHODS

Samples of pure benzene, toluene, heptane, hexane, acetone and acetic acid manufactured by Messer Griesheim were obtained and their purity ascertained at 99.9% using standard procedures. Different binary mixtures were prepared from the pure components by mixing at varying volumes of 1 to 0 ml, 7.5 to 2.5 ml, 5 to 5 ml, 2.5 to 7.5 ml and 0 to 1 ml. The Abbe refractometer double prism system (Model 300778) with monochromatic light source of 589 nm for illumination and with accuracy of 0.0001 was used in measuring the refractive indices. The refractometer was calibrated at 20°C using distilled water as well as samples of the five pure fluids used. Using a heating water bath connected to the refractometer, the refractive indices of the pure components and binary mixtures were measured at 20, 40 and 60°C using procedures similar to Bhatia et al. (2002). Results were replicated to ensure consistency. Deviations of the measured and estimated results were determined using the following equations:

$$D = cal_i - exp_i \qquad (8)$$

$$AAD = ABS\left\{\frac{1}{N} \sum_{I=1}^{N} calc_i - exp_i\right\} \qquad (9)$$

Where "exp_i" is the experimental value, "$calc_i$" is the calculated value for point *i* and *N* is the number of points.

RESULTS AND DISCUSSION

The temperature-dependent modified Arago-Biot mixing rule, Equation (6), accounts for the non-ideal molecular interactions which occurs during mixing. This should represent an improvement over Gladstone-Dale, Arago-Biot and other similar relations. Table 1 gives some of the physical properties of the pure components used for the

Table 1. Physical properties of selected pure compounds.

Compounds	Purity (%)*	Boiling point, (°C)	Refractive index at (20°C)
benzene	99.90	80.1	1.5000
toluene	99.90	110.6	1.4900
heptane	99.50	98.0	1.3800
hexane	99.50	69.0	1.3700
acetic acid	99.90	118.0	1.3700
acetone	99.95	56.0	1.3600

*Supplied by Messer Griesheim.

Table 2. Refractive Index of benzene + toluene at 20°C.

y_i	Experimental (This work)	Lorentz-Lorenz	Weiner	Heller relation	Gladstone-Dale	Arago-Biot (Calculated)	Modified Arago-Biot
0.00	1.4900	1.4900	1.4900	1.4900	1.4900	1.4900	1.4900
0.25	1.4937	1.4909	1.4909	1.4909	1.4921	1.4925	1.4937
0.50	1.4962	1.4949	1.4949	1.4949	1.4945	1.4950	1.4962
0.75	1.4988	1.4989	1.4989	1.4989	1.4972	1.4975	1.4987
1.00	1.5000	1.5000	1.5000	1.5000	1.5000	1.5000	1.5000

Table 3. Refractive Index of Heptane + Hexane mixture at 40°C.

y_i	Experimental (This work)	Lorentz-Lorenz	Weiner	Heller relation	Gladstone-Dale	Arago-Biot (Calculated)	Modified Arago-Biot
0.00	1.3599	1.3600	1.3600	1.3599	1.3600	1.3600	1.3612
0.25	1.3637	1.3609	1.3609	1.3609	1.3625	1.3625	1.3637
0.50	1.3662	1.3649	1.3649	1.3649	1.3650	1.3650	1.3662
0.75	1.3688	1.3689	1.3689	1.3689	1.3675	1.3675	1.3687
1.00	1.3698	1.3700	1.3700	1.3700	1.3700	1.3700	1.3712

Table 4. Refractive Index of Heptane + Acetic Acid at 20°C.

y_i	Experimental (This work)	Lorentz-Lorenz	Weiner	Heller relation	Gladstone-Dale	Arago-Biot (Calculated)	Modified Arago-Biot
0.00	1.3700	1.3700	1.3700	1.3700	1.3700	1.3700	1.3700
0.25	1.3737	1.3709	1.3709	1.3709	1.3746	1.3725	1.3736
0.50	1.3763	1.3749	1.3749	1.3749	1.3772	1.3750	1.3762
0.75	1.3787	1.3789	1.3789	1.3789	1.3788	1.3775	1.3787
1.00	1.3800	1.3800	1.3800	1.3800	1.3800	1.3800	1.3800

experiments as obtained in literature and confirmed during calibration.

Tables 2 to 6 and Figures 1 to 6 shows the results obtained from the experiments. A close observation of these results shows that refractive indices of the pure liquids and mixtures decreased as temperature increased. This agrees with results of previous researchers such as Bhatia et al. (2002), Mehra (2003) and Navendra et al (2011) and can be attributed to the changes in fluid density with temperature. At higher temperatures, liquid dense decreases, causing light to travel faster in the medium resulting in lower refractive index. The variation of refractive indices with temperature can also be attributed to the structural changes which occur during

Table 5. Predictive Refractive Index correlation at varying mole fractions.

$y_i + y_j$	a	b	c
B + T	-0.0056	0.0156	1.4800
Hep + Hx	-0.0054	0.0154	1.3600
Hx + Ac	-0.0053	0.0153	1.3500
Hep + Ac	-0.0054	0.0154	1.3600
AcA + Ac	-0.0053	0.0153	1.3500

$B = benzene, T = toluene, Hp = heptane, Hx = hexane,\ Ac = acetone,\ AcA = acetic\ Acid$

Table 6. Predictive Refractive index correlation at varying temperatures (°C).

$y_i + y_j$	K	$x_1 = 0$	$x_1 = 0.25$	$x_1 = 0.5$	$x_1 = 0.75$	$x_1 = 1.0$
				d		
Be + To	-0.0005	1.5000	1.5037	1.5062	1.5087	1.5100
Hep + Hx	-0.0005	1.3800	1.3837	1.3862	1.3887	1.3900
Hx + Ac	-0.0005	1.3700	1.3737	1.3762	1.3787	1.3800
Hep + Ac	-0.0005	1.3800	1.3837	1.3862	1.3887	1.3900
AcA + Ac	-0.0005	1.3700	1.3737	1.3762	1.3787	1.3800

$Be = Benzene, To = Toluene, Hp = heptane, Hx = Hexane,\ Ac = Acetone,\ AcA = Acetic\ Acid$

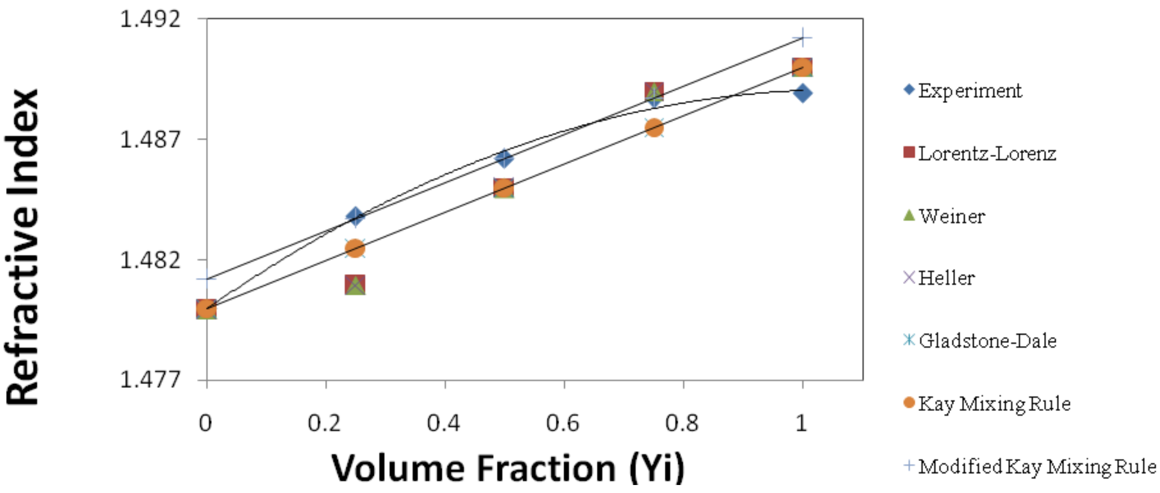

Figure 1. Refractive index versus volume fraction of benzene-toluene at 40°C.

mixing. The experimental results were also used to validate the commonly used mixing rules and the modified Arago-Biot equation. The results show that all estimated refractive indices using the mixing rules were reasonably close to measured values for the binary mixtures.

Furthermore, all the mixing rules considered showed remarkable changes in refractive indices of the mixtures with increasing temperature between 20 and 40°C except the Hexane-Acetone and Heptane-Acetic Acid mixture which were almost constant. This could be as a result of vaporization of acetone and hexane at temperatures close to 56 and 69°C, their boiling points respectively. However, mixtures which contain alkanes were not expected to exhibit structural changes at elevated temperatures between 40 and 60°C, in line with the observation by Mehra (2003) that no effect of increase in chain length was observed in alkanes and alkanols.

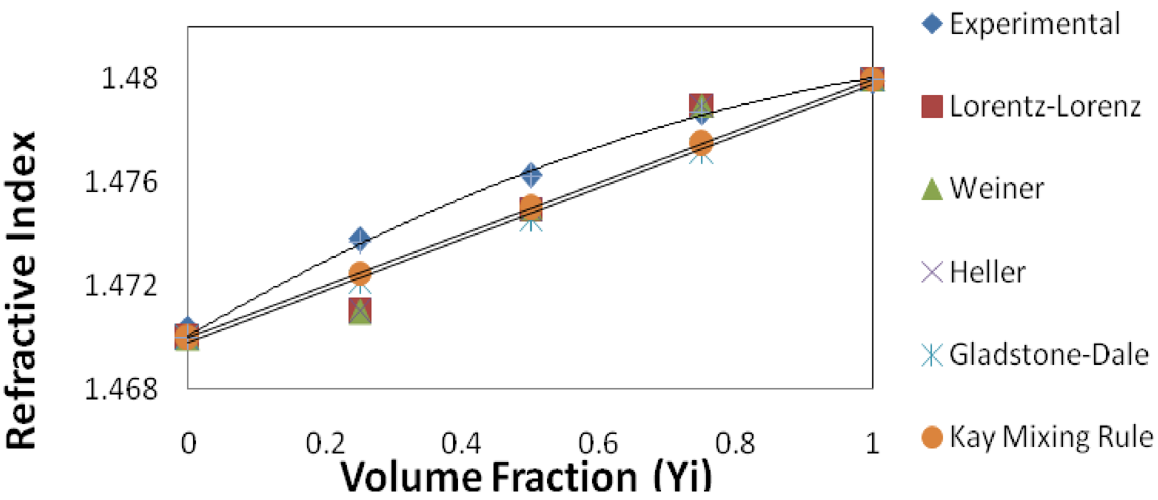

Figure 2. Refractive index versus volume fraction of benzene-toluene at 60°C.

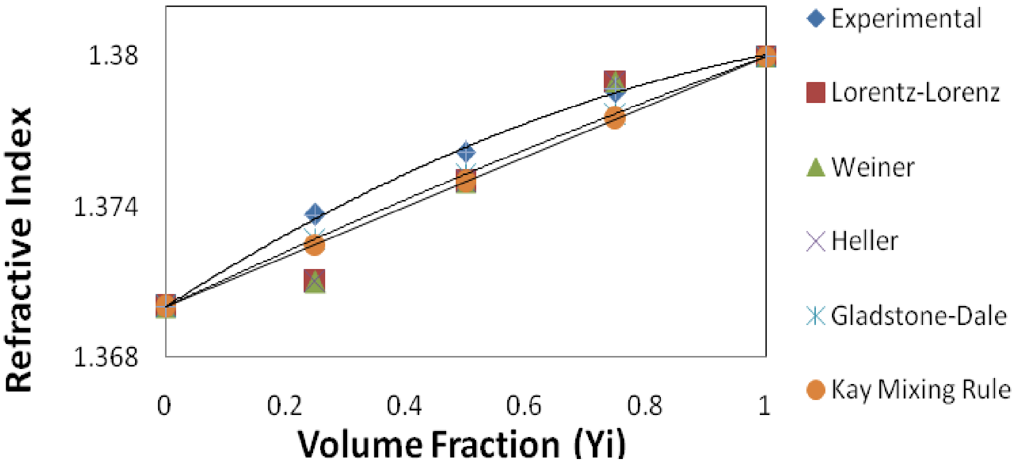

Figure 3: Refractive index versus volume fraction of heptane-hexane at 20°C.

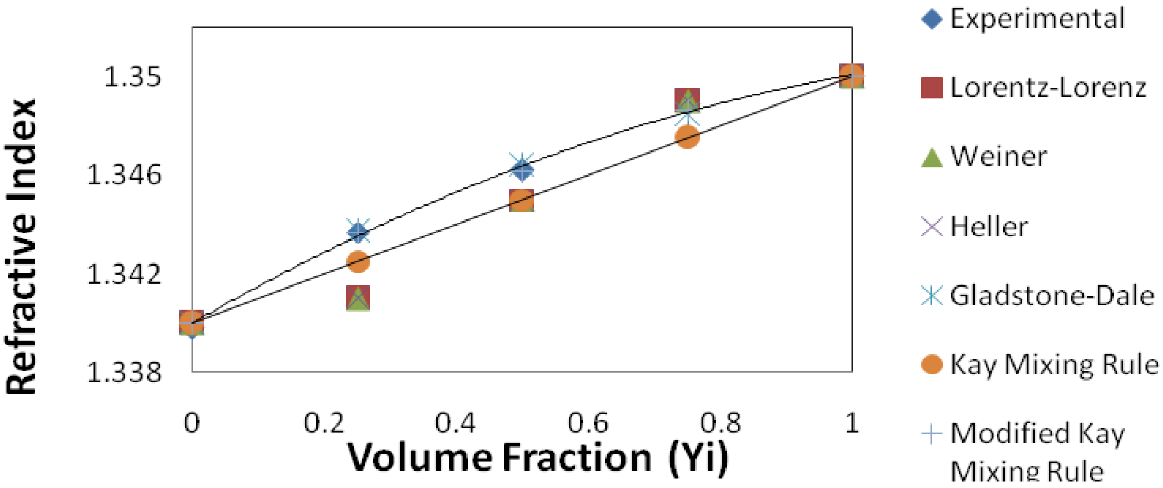

Figure 4. Refractive index versus volume fraction of hexane-acetone at 60°C.

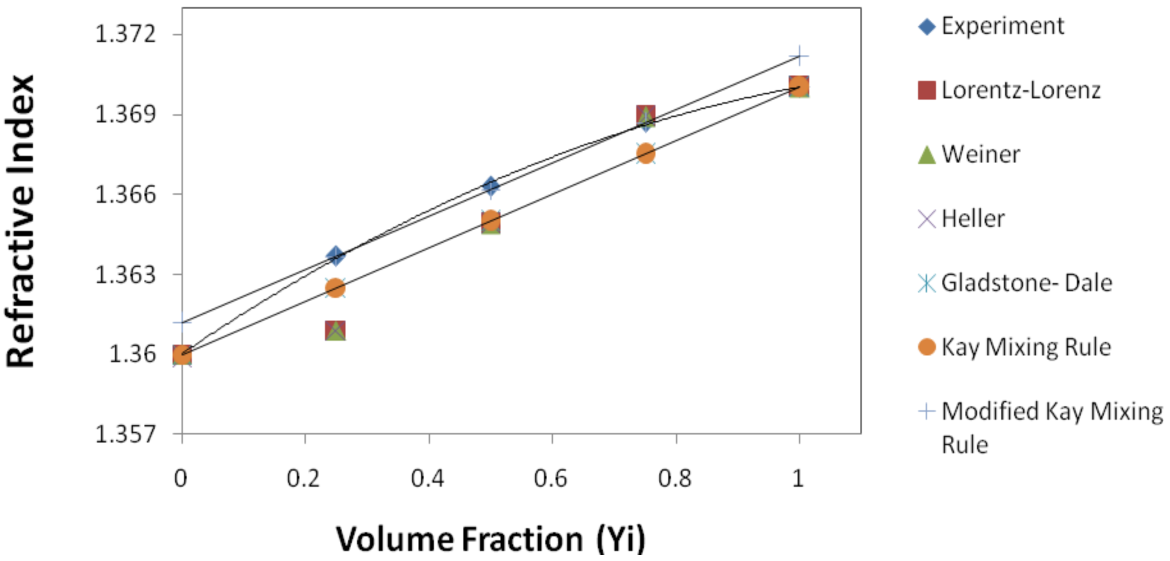

Figure 5. Refractive index against volume fraction of heptane-acetone at 40°C.

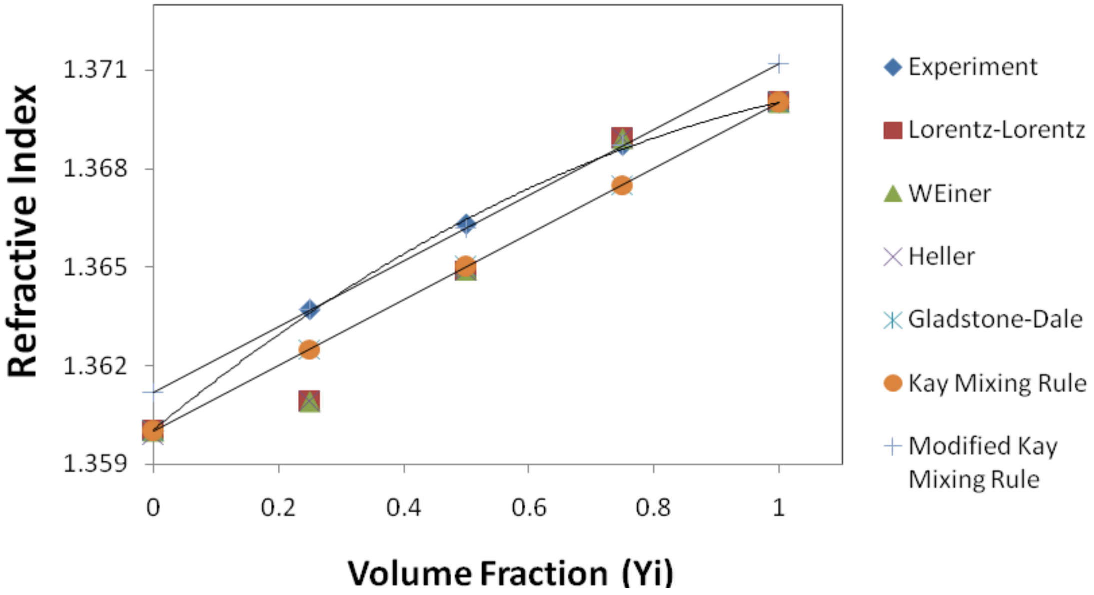

Figure 6. Refractive index versus volume fraction of acetic acid-acetone at 20°C.

Using the experimental data, the refractive indices of the selected binary mixtures at 20°C were related to volume fraction by equation (10):

$$n = ay_i^2 + by_i + c \tag{10}$$

Where, y_i is volume fraction of component 'i', while a, b and c are empirical constants as defined in Table 4.

Furthermore, the variation of refractive index with temperature was clearly established in this study in agreement with previous researchers (Bhatia et al., 2002). Therefore, we propose the estimation of the refractive indices of the mixtures at elevated temperatures using Equation (11):

$$n_t = d + KT \tag{11}$$

Where, K = Temperature correction factor = 0.0005/°C, d = Constant as given in Table 5, n_t = Refractive index at any temperature T °C other than base temperature.

Conclusion

Based on this work, the following conclusion can be made:

(1) The refractive indices of selected binary mixtures have been determined and presented.
(2) Refractive indices of the pure components and binary mixtures investigated in this study decrease with increasing temperature. Similar trends are expected in other similar compounds.
(3) The modified Arago-Biot mixing rule which includes temperature effects is simple to use and has wider range of application than some of the existing relations in literature. Therefore, an accurate mixing rule should not only be volume fraction-dependent, but explicit in temperature.

Conflict of Interest

The authors have not declared any conflict of interest.

ACKNOWLEDGEMENT

This study was supported by the Shell Petroleum Development Company, Nigeria through the Shell Chair Office at the University of Ibadan.

NOMENCLATURE:

n_m = refractive index of mixture ,
n_1, n_2 = Refractive index of pure components,
$\emptyset_1$ and $\emptyset_2$ = volume fractions,
w_1 and w_2 = weight fractions ,
ρ_m = density of mixture,
ρ_1, ρ_2 = density of pure components ,
K= Temperature correction factor,
n = Refractive index ,
n_D = Refractive index of mixture,
ρ = Density of the mixture,
ρ_i = Density of component 'i' ,
M_i = Sum of components mass ,
V = Total volume occupied by fluid mixture,
y_i = mole fraction of component 'i' ,
m_{dn} = Mixing deviation for pure components
n = Refractive index of mixture,
n_t = Refractive Index of component mixture at a specific temperature ,
n_{t_i}' = Temperature dependent Refractive index of component 'i',
T = Temperature, oC .

REFERENCES

Ali A, Tariq M (2006). Thermodynamic and transport behaviour of binary liquid mixtures of benzyl alcohol with monocyclic aromatics at 303.15 K. J. Mol. Liquids. 128:50-55.
Ali A, Nabi F, Itoo FA, Tasneem S (2008). Volumetric, Ultrasonic, viscometric and refractive index behaviour of binary mixtures of styrene with ethylalcohol and chlorobenzene at different temperatures (T = 298.15K to 313.15K). J. Mol. Liquids. 143:141-146.
Andrew WV, Khoo TBK, Jacobs DT (1986). Testing the Lorentz-Lorenz relation in the near-critical binary fluid mixture isobutyric acid and water. J. Chem. Phys. 85(7):3985-3991.
Bhatia SC, Tripathi N, Dubey GP (2002). Refactive indices of binary liquid mixtures of decane+benzene and hexadecne +benzene or + hexane at 303.15, 308.15 and 313.15 K. India J. Chem. 41A:266-269.
Brocos P, Pineiro A, Bravo R, Amigo A (2003). Refractive indices, molar volumes and molar refractions of binary mixtures: concept and correlations. Phys. Chem. 5:550- 557.
Ebatco (Exponential Business and Technologies Company) (2013). Refractive Index Measurements to Compare Chemical Purity Retrieved November 8, 2013 from http://www.ebatco.com
Leron RB, Allan N, Meng-Hui L (2012). Densities and refractive indices of the deep eutectic solvents (chlorine + ethylene glycol or glycerol) and their aqueous mixtures at the temperature ranging from 298.15 to 333.15K. J. Taiwan Inst. Chem. Eng. 43:551-557.
Meenachi M, Krishnamurthi P (2013). Theoretical prediction of refractive index of phenol with hydrocarbons at 303K. Mechanica Confab. 2(2):85-92.
Mehra R (2003). Application of refractive index mixing rules in binary systems of hexadecane and heptadecane with n-alkanols at different temperatures Proc. Indian Acad. Sci. Chem. Sci. 115(2):147-154.
Navendra K, Narayanamurthy P, Srinivasu Ch (2011). Refractive indices of binary liquid mixture at different temperatures. Asian J. App. Sci. 4:535-541.
Rilo E, Domínguez-Pérez M, Vila J, Segade L, García M, Varela LM, Cabeza O (2012). Easy prediction of the refractive index for binary mixtures of ionic liquids with water or ethanol. Elsevier J. Chem. Thermo. 47:219-222.
Rushton JH (1955). Fundamentals of Mixing in Petroleum Refining. Proceedings Fourth World Petroleum Congress. Paper 3. Section III/B.
Sharma S, Patel P, Rignesh SP, Vora JJ (2007). Density and comparative refractive index study on mixing properties of binary liquid mixtures of eucalyptol with hydrocarbons at 303.15, 308.15 and 313.15K. E-J. Chem. 4(3):343-349.
Singh S (2002). Refractive Index Measurement and its Applications. Physica Scripta. 65:167-180.
Vural US, Muradoglu V, Sedat V (2011). Excess Molar Volumes and Refractive Index of Binary Mixtures of Glycerol + Methanol and Glycerol + Water at 298.15K and 303.25K. Bull. Chem. Soc. Ethiop. 25(1):111-118.
Wankhede DS (2011). Refractive Indices for Binary Mixtures of Propylene Carbonate. Int. J. Chem. Res. 2(2):23-26.

academicJournals

Vol. 9(4), pp. 65-70, April, 2015
DOI: 10.5897/AJPAC2015.0617
Article Number: 2D11C6C52529
ISSN 1996 - 0840

http://www.academicjournals.org/AJPAC

African Journal of Pure and Applied Chemistry

Full Length Research Paper

Oxidation of acha (*Digitaria exilis*) starch using 3.5% active chlorine sodium hypochlorite

S. Isah*, A. A. Oshodi and V. N. Atasie

Bells University of Technology, Nigeria.

Received 15 February, 2015; Accepted 17 March, 2015

Acha (*Digitaria exilis*) starch was chemically modified using sodium hypochlorite (3.5% active chlorine) as oxidative agent. The physicochemical properties of the native acha starch and oxidized derivative were investigated. Oxidation improved the water and oil absorption capacity of the native acha starch and also the emulsion capacity was significantly improved. The bulk density, foam capacity and solubility reduced upon oxidation. The granule morphologies investigated using scanning electron microscopy showed significant difference in the ratio of crystalline and amorphous regions. However, oxidation of native acha starch did not affect the shape, appearance and structural arrangement of the starch granules. The granules were polygonal in shape with size range of 6 to 8.57 µm. The infra spectra showed additional band at 3600 cm^{-1} for the oxidized derivative indicating hydroxyl group stretching vibration of carboxylic acid. This indicates that the oxidation of native acha starch was successfully carried out. Improved physicochemical properties impacted upon oxidative modification is quite desirable in impacting greater stability and less retrogradation and seneresis of the native acha starch. Thus, oxidized acha starch will find suitable applications in food, pharmaceutical, paper and textile industries as good dispersants, emulsifying agent, surface sizing, adhensive, disintegrants, excipients and preparation of biopolymer based flocculants.

Key words: Modified starch, starch oxidation, physicochemical properties, scanning electron microscopy, starch granules.

INTRODUCTION

The genus *Digitaria* referred to as fonio, family Poaceae, is one of the smallest cereal grains indigenous to most West African countries. It is one of the primary cereals of southern Sudan and Ethiopia. It is classified as millet but unlike other millets, it is low in protein (Jideani and Akingbala, 1993). They are consumed whole or milled into flour and can be processed into a variety of preparations such as gruels, porridges, beverages etc. (Coda et al., 2010).

To obtain oxidized starch, the most common approach is treating the native starch with a variety of oxidizing agents such as alkali metal hypochlorite. Oxidation improves whiteness and reduces microbiological content. In addition, the hydrogen bonding reduces the tendency to retro-gradation producing soft- bodied gels of high clarity.

The oxidation reaction are controlled by many factors such as the amount of alkali metal hypochlorite used, the

---

*Corresponding author. E-mail: slyshehu@yahoo.com

pH, the temperature, and the use of metal and/or bromide ions as catalyst. The oxidative reactions lead to the introduction of carboxyl and carbonyl groups, and to the degradation of the starch molecule.

The degradation of the starch molecule during oxidation leads to a lower viscosity of a solution (or dispersion) of the oxidized starch, which is usually desired of an oxidized starch. It has been found that the degradation occurs to a farther extent at neutral pH of about 7 to 7.5 than at alkaline pH such as pH of 9 or higher. In other words, in order to obtain an optimal yield of oxidized starch providing a dispersion of low viscosity, the oxidation reaction should preferably be carried out at neutral pH.

In practice, the pH during oxidation of starch using an alkali metal hypochlorite is chosen at 8.5 or higher, dependent mostly on the desired viscosity of the oxidized starch. Alkali metal hypochlorite often used as oxidizing agent is relatively cheap and large oxidizing power. The reaction temperature at which the starch is treated with an oxidizing agent is preferably chosen between 20 and 50°C.

The duration of alkaline treatment lasts at least 30, more preferably at least 60 min. Oxidized starch is used in the paper industry as coating binders, surface sizing and adhesives. It is also as emulsifying agent, protective colloid for providing desired stability and also to improve weaving operation in the textile industry by improving abrasion resistance of the warp yarn sizing. Arabic gum may be substituted in confectioneries by an oxidized starch to provide excellent stability of the food product, leading to a more clear food product.

MATERIALS AND METHODS

Oxidation of acha starch

25 g of starch was dissolved into 100 ml of distilled water and the pH of starch solution adjusted to 10 to 11 with sodium hydroxide solution. The starch slurry was heated to a temperature of 30°C and 20 ml of sodium hypochlorite solution (3.5% active chlorine) added to the starch solution dropwise over a period of 20 min with stirring. During the addition of the reagent and the course of reaction the pH of the slurry was maintained at the desired value with NaOH or HCl solution. The mixture was stirred under the defined conditions above (temperature of 30°C) and then terminated after 2 h by addition of sodium metabisulphite. Filtered and suspended in distilled water and the pH adjusted to 6.5 to 7.0 and oven dried at 50°C.

Determination of physicochemical properties

Solubility

The native starch and modified starch samples (2 g each) were suspended in 20 ml of distilled water. Then heated to 70°C for 30 min with continuous shaking. The mixture was then centrifuged at 4000 rpm for 15 min. An aliquot of supernatant (5 ml) was evaporated at 105°C and weighed. The solubility of starch is the ratio in mass (g) of the dried supernatant to the initial mass (g) of dried starch.

Water and Oil absorption capacity

1 g of native and modified starch was weighed into test tubes. 10 ml of distilled water (and 10 ml of groundnut oil in the second test tube) were added, and then heated in a water bath at 60°C for 30 min. The starch slurry was centrifuged at 1000 rpm for 15 min and the supernatant carefully decanted and the weight of the starch paste taken.

WAC/OAC= weight of starch paste/weight of dry starch sample.

Bulk densities of native and modified starch

2 g each of native Acha starch and the modified starch were placed in a 10 ml measuring cylinder and the volume occupied by the sample without tapping recorded. The bulk density is the ratio of the weight to volume occupied.

The pH of starch

The pH of 1% w/v slurry of both the native starch and modified starch were determined using a pH meter.

Least gelation concentration of starch

8 samples each for native and modified starches (1 to 16% w/v) were prepared in test tubes with 5 ml of distilled water. The starch solutions were mixed using magnetic stirrer for 5 min and heated for 30 min at 80°C in a water bath followed by rapid cooling under running cold water. Further cool at 4°C for 2 h. Least gelation concentration was determined as that conc. when the samples from the inverted test tube did not fall down or slip.

Pasting properties of the starch

The pasting property of native starch and modified sample was carried out using Brookfield viscometer.

Foam capacity of starch

2 g of native Acha starch and each of modified starch were homogenized in 100 ml of distilled water using a magnetic stirrer for 5 min. The homogenate was poured into a 250 ml measuring cylinder and the volume occupied was recorded after 30 s. The foam capacity is expressed as the percent increase in volume.

Emulsion capacity of starch

2 g of native and modified acha starch were dispersed in 25 ml of distilled water using a magnetic stirrer for 30 s. After complete dispersion, 25 ml of vegetable oil (groundnut oil) was added gradually and the mixing continued for another 30 s. Then centrifuged at 1600 rpm for 5 min. The volume of oil separated from the sample was read directly from the tube. Emulsion capacity is the amount of oil emulsified and held per gram of sample.

Starch granules morphology

The starch granule morphology of both the native starch and modified starch were obtained using scanning electron microscopy (sem).

Table 1. Physicochemical properties.

Properties	NAS	OAS
Solubility (g)	10.24±0.02	9.32±0.04
Water absorption capacity (%)	488	499
Oil absorption capacity (%)	122	115
Bulk density (g/ml)	0.41±0.03	0.44±0.01
pH	6.85	6.40
Foam capacity (%)	4.0±0.00	3.2±0.02
Emulsion capacity (%)	36±0.02	39±0.03
Viscosity (cP)	31.5	20.2

NAS= Native acha starch ; **OAS**= Oxidized acha starch.

RESULTS AND DISCUSSION

Solubility

The results of solubility of native acha starch (NAS) and oxidized starch (OAS) are shown on Table 1. The solubility expressed as gram per 100 g of starch (g/100 g) reduced from 10.24 value observed with the native acha starch to 9.32 for oxidized starch. The decrease in solubility of oxidized samples is probably due to introductions of bulky functional groups reducing the mobility of starch molecules. This pattern agreed with the results of Olu-owolabi et al. (2014). Thus, modifications altered this physical property (that is, solubility) of native acha starch.

Water absorption capacity

The water absorption capacity of native acha starch and chemically modified sample is presented in Table 1. Oxidation improved water absorption capacity of native acha starch. This may be attributed to the incorporation of carboxyl functional groups on the starch molecules which enhanced binding capacity more than the native starch. The increase in water absorption capacity following oxidation is very important especially in the application of this starch either as a drug carrier or disintegrant in tablets and capsule formulation (Emeje et al., 2012).

Oil absorption capacity

The result of oil absorption capacity of native acha starch and modified sample is presented in Table 1. The values expressed as percentage varied from 122 observed with native acha starch to 115 observed for oxidized sample. This may be attributed to the functional groups incorporated onto the starch molecule following chemical modification. This agrees with the report of Sathe and Salunkhe (1981) that acetylation and oxidation do not improve oil absorption capacity of great northern bean. This increase in starch crystallinity restricted access of oil into the granule of the starch. This is because chemical modification is thought to occur in the amorphous region of the starch molecules leading to increase in starch crystallinity.

pH of starch slurry

The result of pH of starch slurries of native and modified acha starch are presented in Table 1. The pH values reduced from 6.85 to 6.40. A reduction on pH value was observed following modification by oxidation. Reduction in pH values of oxidized samples may be attributed to the incorporation of acetyl functional group to the starch molecule thereby increasing the acidity of starch molecules.

Bulk density

The bulk density of native acha starch and modified sample are presented on Table 1. The bulk density values were in the range of 0.39 to 0.50. A reduction of bulk density was observed with all chemical modifications of the native acha starch. The least bulk density was observed with the acid thinned sample (0.39). The reduction in bulk density might be attributed to increased crystallinity following chemical modification. Increase crystallinity is characteristic of more ordered state and this might impact greater stability on the modified samples. Thus retrogradation of native acha starch as well as seneresis may be improved upon modification. This reduction in bulk density is in agreement with Emeji et al. (2012). This improved physical property following chemical modification of native acha starch is desirable in food and pharmaceutical applications as good dispersant and preparation of biopolymer based flocculants.

Foam capacity

The result of foam capacity of native acha starch and

Table 2. Least gelation concentration (%).

Concentration (%)	NAS	OAS
2	Viscous	viscous
4	Viscous	Viscous
6	Gel	Gel
8	Gel	Gel
10	Gel	Gel
12	Gel	Gel
14	Gel	Gel
16	Gel	Gel

NAS**=** Native acha starch; **OAS** = Oxidized acha starch.

modified samples are presented in Table 1. The foam capacity of oxidized sample was reduced to 3.2% from 4% observed with native acha starch. Reduction in foam capacity following oxidation could find application as an emulsifier in the food industries (Ihegwuagu et al., 2009).

Emulsion capacity

The emulsion capacity of native acha starch and oxidized samples is presented on Table 1. The emulsion capacity increased in the modified samples from 36 to 39%. This suggests that chemically modified acha starch are better emulsifying agent due to the introduction of functional groups in the starch molecules increasing the binding force of the starch granules.

Least gelation concentration

The gelation properties of native acha starch (NAS) and oxidized samples are presented in Table 2. The least gelation concentration remained at 6%.

Starch pasting properties

The pasting properties of NAS and modified samples are presented in Table 1. These are shown as viscosities (Cp) at room temperature using Brookfield Viscometer. The pasting viscosities of modified samples were reduced from 31.5 centipoise for native acha starch to 20.2 centipoise for oxidized sample. The pasting viscosity reduced by about 30% on modification. In such instances where high content of starch is desirable in order for the starch to be able to form a gel as in wine gums and liquorice the pasting property of native starch would be too viscous during heating. In such applications, we can take advantage of oxidized starch. Also in instant soups compositions, thin boiling starches are often used as filler.

Starch granule morphology

Starch is stored in most green plants as minute granules in the leaves, stems, roots, fruits and seeds. Such starch is stored traditionally for the future use of the plant. The granule morphology of NAS and modified samples are shown in Figure 1. These morphologies were investigated using scanning electron microscopy at 15kv accelerating voltage and 2500 magnification each. Though increased crystalline region is observed on modifications, it is obvious that modifications may not have destroyed the shape, appearance and structural arrangements of the starch. The starch granules retain its polygonal shape with sizes ranging from 6 to 8.57 µm.

Starch utilization as a food or feed relate to its physical and chemical properties. The solubility of starch starts with swelling in the gel or amorphous region leaving the crystalline structure unaffected. But with higher temperature, the crystalline region melts or dissolves and the entire crystalline structure are destroyed. With increased crystallinity from cross-linked and acid treated modifications, less solubility and improved stability are expected from these modified samples.

Infra red (IR) spectra

The infra red (IR) spectra of NAS and modified derivative are presented on Figures 2 and 3 respectively. The infra red spectra have similar peaks, except for the additional peak at 3600 cm^{-1} on Figure 3 which is ascribed to the –OH stretching vibration of the carboxylic acid groups. These bands confirm that modifications of NAS were successfully carried out.

Conclusion

Oxidation of NAS was successfully carried out. The physicochemical properties of NAS and modified derivative were determined. Chemical modifications enhanced emulsion capacity, water absorption capacities

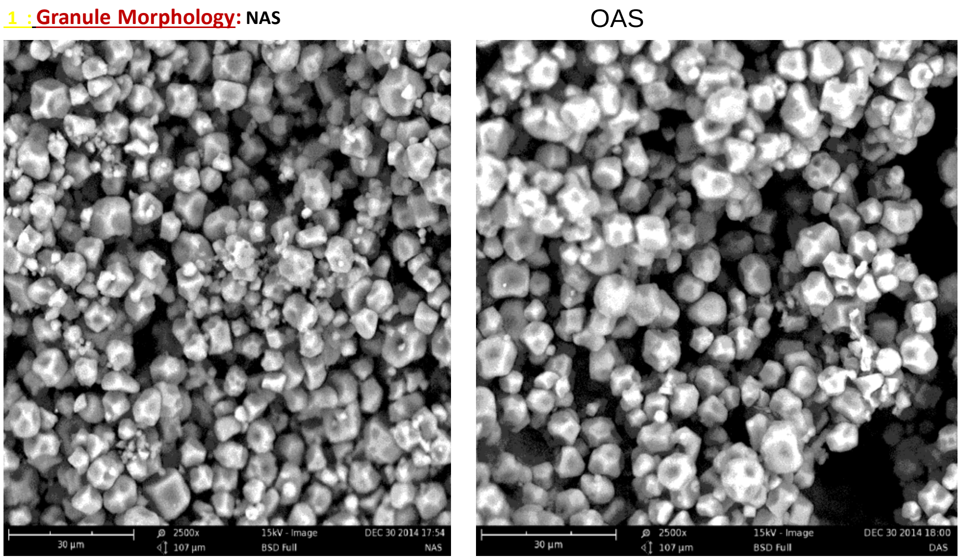

Figure 1. Comparison of Granule morphology NAS vs OAS.

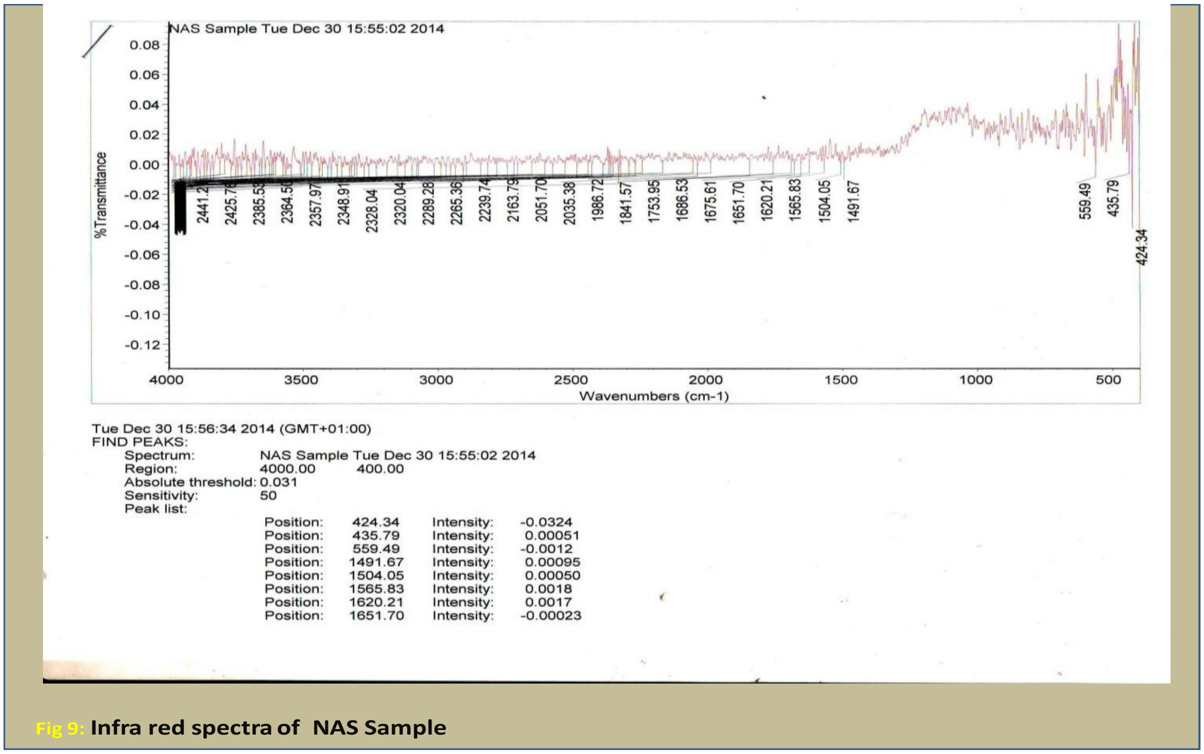

```
Tue Dec 30 15:56:34 2014 (GMT+01:00)
FIND PEAKS:
     Spectrum:            NAS Sample Tue Dec 30 15:55:02 2014
     Region:              4000.00        400.00
     Absolute threshold:  0.031
     Sensitivity:         50
     Peak list:
                          Position:    424.34    Intensity:   -0.0324
                          Position:    435.79    Intensity:    0.00051
                          Position:    559.49    Intensity:   -0.0012
                          Position:   1491.67    Intensity:    0.00095
                          Position:   1504.05    Intensity:    0.00050
                          Position:   1565.83    Intensity:    0.0018
                          Position:   1620.21    Intensity:    0.0017
                          Position:   1651.70    Intensity:   -0.00023
```

Figure 2. Infra red spectra of NAS Sample.

but reduced the paste viscosity, oil absorption and foam capacity. Oxidation improved NAS stability and less retrogradation. Potential applications of modified acha starch include good emulsifying agent, starch thickened sauces, soups, paper binding and pharmaceutical drug carriers and disintegrants including paper surface sizing and adhensives.

Conflict of Interest

The authors have not declared any conflict of interest.

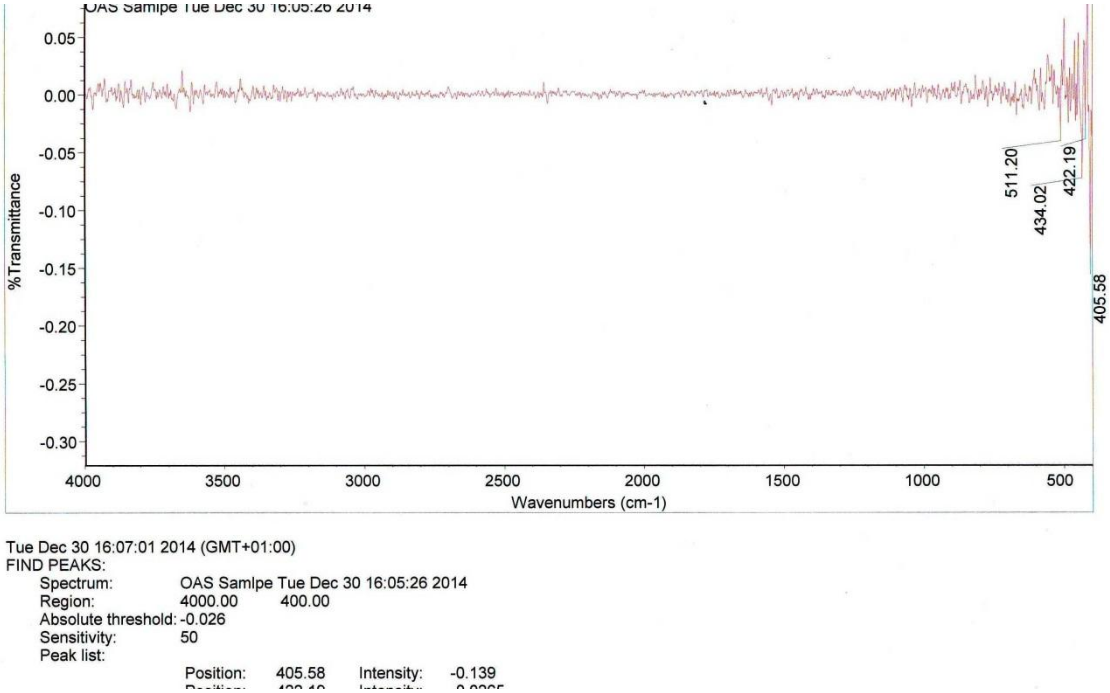

Tue Dec 30 16:07:01 2014 (GMT+01:00)
FIND PEAKS:
Spectrum: OAS Samlpe Tue Dec 30 16:05:26 2014
Region: 4000.00 400.00
Absolute threshold: -0.026
Sensitivity: 50
Peak list:
Position: 405.58 Intensity: -0.139

Figure 3. Infra red spectra of OAS sample.

REFERENCES

Coda R, Cagno RD, Edema MO, Nioeli L, Gobbetti M (2010). Exploitation Of Acha (*Digitaria exillis*) And Iburu (*Digitaria Iburua*) Flours: Chemical characterization and their use for sourdough fermentation. Food microbial J. 27:1043-1053.

Emeje M, Kaita R, Isimi C, Buragohain A, Kunle O, Ofoefule S (2012). Synthesis, physicochemical characterization, and functional properties of an esterified starch. Afr. J. Food Agric. Nutr. Dev. 65:369-374.

Ihegwuagu EN, Omojola OM, Emeje MO, Kunle OO (2009). Isolation and evaluation of some physicochemical properties of Parkia Biglobosa starch. Pure Appl. Chem. 81(1):97-104.

Jideani AI, Akingbala JO (1993). Some physicochemical properties of acha (*Digitaria exilis* Stapf) and iburu (*Digitaria iburua* Stapf) grains. J. Sci. Food Agric. 65(4):465-476.

Olu-Owolabi BI, Olayinka OO, Adegbemile AA, Adebowale KO (2014). Comparison of functional properties between native and chemically modified starches from acha (*Digitaria* stapf) grains. J. Food Nutr. Sci. 5:222-230

Sathe SK, Salunkhe DK (1981). Isolation, partial characterization and modification of the great Northern bean (*Phaseolus vulgaris* L.) Starch. J. Food Sci. 46:617-621.

academicJournals

Vol. 9(4), pp. 71-80, April, 2015
DOI: 10.5897/AJPAC2015.0610
Article Number: 0BC22C952530
ISSN 1996 - 0840

http://www.academicjournals.org/AJPAC

African Journal of Pure and Applied Chemistry

Full Length Research Paper

Reversal of plasticity of acid leached kaolinitic clays from Mukurwe-ini

Dickson Andala[1] and Wachira David Maina[2]*

[1]Department of Chemistry, Multimedia University of Kenya, Kenya.
[2]Department of Chemistry, Kenyatta University, Kenya.

Received 22January, 2015; Accepted 24 March, 2015

This study aimed at finding out whether the property of plasticity of acid leached clays can be reversed by treatment with a suitable base. Studies were carried out on representative samples, which were taken from iron bearing clays from Mukurwe-ini, Nyeri County in Kenya (Latitude 00°34´00´´S, Longitude 37°03´00´´E). Characterization of the clay was done in its natural form, and after acid treatment, to determine its mineralogical and chemical composition. Natural clay was refluxed with sulphuric and hydrochloric acids of different concentrations at 100 and 200°C for 2 h followed by thorough washing with distilled water to remove the acid matrix. Atomic absorption spectroscopy, X-ray fluorescence spectroscopy, and X-ray diffraction, analysis techniques were used to determine the physico-chemical characteristics of natural and acid leached clays. The results indicate that SiO_2, Al_2O_3, and Fe_2O_3 are the major components of Mukurwe-ini clay, MgO, CaO, K_2O, TiO_2, MnO, and Na_2O are present in trace amounts. XRD characterization shows that Mukurwe-ini clays consist primarily of quartz, kaolinite, albite, and microcline minerals. Iron content was drastically reduced in the acid washed samples and X-ray diffraction (XRD) mineralogical analysis of base acid-activated clays showed enhanced levels of the mineral kaolinite in comparison to acid-activated clays (5.3 to 15.7%) a clear indication that the natural properties of the acid washed clay were restored by base treatment of acid washed samples. The Atterberg limits of the base treated samples closely compared with those of the natural clays.

Key words: Clay minerals, Atterberg limits, and plasticity.

INTRODUCTION

Plasticity is the property that makes a body to show changes of its shape without rupture when an external force is exerted on it, so that when the deforming force is removed the acquired shape is maintained (Andrade et al., 2010; Keller, 1979). Plasticity is a very important property of clays in that distinguishes clay from other similar sized colloidal particles. An understanding of the factors, which determine it in soils, will aid in the interpretation of test data, and lead to a better understanding of the performance of clay soils in applications such as in ceramics and engineering. The factors that affect the plasticity of a soil are also likely to affect most of its other properties that are of interest to the engineers (Dumbleton and West, 1966). Plasticity in clays is attributable to a multiplicity of inter-related factors, which in most cases act together, that it is hard to

---

*Corresponding author. E-mail: Mainawachira14@yahoo.com

pinpoint at a single factor as the cause of this important ceramic property. However, water of plasticity plays a key role in defining this property. Other factors that do affect clay plasticity include particle size, specific surface area, water characteristics, mineralogical composition, dispersion state of particles, and ceramic body temperature (Andrade et al., 2010). A keen study of structure of clays reveals that these minerals hold water in various forms. Water is confined in the pores in the clay particles by capillarity action. Adsorbed water is held in the interlamella layer of the sheet silicates. Either of these two forms of water is easily lost by drying or heating the clay between 100 to 200°C and it is easily regained under ordinary conditions. Water is also held in form of hydroxyls. Hydroxyl water is driven off from the clay minerals at elevated temperatures between 400 to 700°C, dehydroxylation results in oxidation of Fe^{2+} to Fe^{3+} hence the colorization of the clays at elevated temperatures (Stucki et al., 1984a). Chemical and physical properties of clay minerals are integrally linked to how the clay surface interacts with the different forms of water present in the minerals. Examples of such properties include; all of the adsorptive catalytic and cation exchange reactions, shrink-swell phenomena, plasticity, and catalysis (Schoonheydt and Johnson, 2006). Moisture content influences strongly the engineering properties of clays. When clays are subjected to high temperatures, they lose adsorbed and hydration water leading destruction of the clay structures (Gulgun, 2011). Cao et al. (2011) did a study on the effect of low concentration of NH^{4+} on adsorption of vermiculite from Hebei province, China and found that indeed the ammonium ion is adsorbed on the surface of the minerals. The plasticity index gives an indication of the degree of plasticity shown by clay body and is often be correlated with properties such as specific surface area, dry strength, and rheological behaviour. The plastic limit gives an estimate of the sorptive properties of clays and may be correlated with shrinkage on drying (Bain, 1971). Plasticity measurement is usually evaluated by means of the water of plasticity (Keller, 1979). The tests for Atterberg limits were developed as a means of distinguishing between clays and other soils. The "liquid limit" is the relatively high water content at which the soil changes from a liquid to a plastic state, and the "plastic limit" designates the relatively low water content at which soil changes from a plastic to a solid state (Dumbleton and West, 1966).

The procedures for determining the liquid and plastic limits are well established and are described in detail in publications of the American Society for Testing and Materials and of the British Standards Institutions (British Standard, 1377: Part 2 1990).The difference in water content between the liquid and plastic limits is defined as the "plasticity index" of the soil. High values of plasticity index mean that the clay is more plastic and compressible, hence the greater the shrinkage characteristics of the soil. The plasticity index has proven to be one of the most useful of all soil indices and is essential to the description of a cohesive soil (Andrade et al., 2010).Atterberg's plasticity index (PI) provides a good aid in the examination of plasticity of ceramic raw materials consisting of clay mixtures and iron oxides.

Presence of inherent impurities has a big impact on the utility of clays. Iron is the fourth-most abundant element in Earth's crust (6% of mass); next to oxygen, silicon and aluminium, its ubiquitous presence in clays should be no surprise (Stucki, 2006; Atkins et al., 2006). In order to make high quality ceramic products, clays with low shrinkage, good plastic properties and long vitrification range are used; however, large amounts of iron affect these vital properties (Grim, 1979). Structural and colloidal iron causes unwanted colour on clays when they are fired (Stucki et al., 1984b). Reduction of iron impurities is therefore of great importance for the usability of clay in many applications, particularly in ceramic, paper and catalysis industries where purity requirement are specifically high. When iron is confined in structural form, low concentrations are often tolerable. In order to make high quality ceramic products, clay with low iron content, preferably less than 1% is desirable (Karoki, 2009). Chemical-treatment remains one of the methods used to reduce the level of iron in clays. The method however leads to loss of clay's natural structural properties such as plasticity that would render the treated materials unusable in many ceramic applications. The acid-treated and cation exchanged clays can be simply regarded as solid acids and act as heterogeneous catalysts. Their obvious benefits include low cost, ease of separation, reduced waste generations and environmental friendliness (Igbokwe et al., 2011). Acid-treated have large surface areas and swelling properties suitable for use in solid supports for inorganic reagents such as potassium permanganate, thallium (III) nitrate and both copper (II) and iron (III) nitrates (Yahiaoui et al, 2003). The process involves acid-activation of the clays with strong mineral acids like HCl, H_2SO_4 and HNO_3.The activated material has improved specific surface area and acidity (Vaughan and Pattrick, 1995). The clays used should be free of iron and other metal ions, which may poison the catalysts. Acid–activated clays have been in use in petroleum industry in catalytic cracking of long chained fractions. They are extensively used in edible oil industry to remove offending smells and to decolorize the oils. White clay is used as filler and coating material in the paper industry, kaolinite minerals are used for this purpose (Grim, 1979). Common clays are used in manufacture of hydraulic cements where tetra calcium aluminiumferrite (C_4AF) makes up 5-15% of normal Portland cement clinkers (Mohamed and Hesham, 2010). The level of iron in clays used in making Portland cement ranges between 0.5-6.0% of clay materials otherwise; the

Table 1. Sampling and coding of samples.

Mine	Sample code	Depth of sample collection (m)	Colour	Texture	Density
A	Muk A1	0.45	Gray with traces of brown hue	Fine grained	Dense
	Muk A2	0.90	Gray with traces of brown hue	fine grained	Dense
	Muk A3	1.50	Gray with traces of brown hue	Silty	Dense
B	Muk B1	0.45	Gray with traces of brown hue	Fine grained	Dense
	Muk B2	0.90	Gray with traces of brown hue	Fine grained	Dense
	Muk B3	1.50	Gray with traces of brown hue	Silty	Dense
C	Muk C1	0.45	Gray with traces of brown hue	Fine grained	Dense
	Muk C2	0.90	Gray with traces of brown hue	Fine grained	Dense
	Muk C3	1.50	Gray with traces of brown hue	Silty	Dense

(Dry density range= 1.75-2.0, Standard penetration test, N-value average =42, hence categorised as dense).

cement product will have undesired colour after calcination process (Neville, 2012).

In agriculture, activated clay catalysts are used as selective adsorbents of non-ionic organics such as aromatics and chlorinated hydrocarbons (Vaughan and Pattrick, 1995). Clays serve as inert carriers of most pesticide without affecting their potency or activity because of their inert nature. Clays for instance, bentonites make good backfill material for underground nuclear-waste repositories because of their inane ability to self-seal and retain contaminants when they are hydrated (Julia and Lawrence, 2011). Clays are extensively used in modification and improvement of road pavements to enhance viscosity and penetration of the soil surface (Grim, 1979).

Clay minerals hold significant amounts of aluminium in their structures. Clay deposits are now in use as alternative source of aluminium because of depletion of traditionally used alumina deposits (Karoki, 2009). The clay used for aluminium extraction should have high aluminium content; kaolinite clays are popular for this reason. It has already been mentioned elsewhere in this literature review that clays have adsorptive abilities and for this reason they find good use in beauty and pharmaceutical industries because they effectively adsorb toxins on the skin, for example talc is used in pastes, ointments and lotions for skin toning. Kaolinite clays are used to cure gastronomic disorders because they can absorb bacteria and other microorganisms in the stomach and intestinal lining of digestive systems.

The emphasis for future work is on advanced clay-based nanomaterials for use in new approaches to sustainable energy, green environment and human health. There is a shift from traditional use of clay-products in ceramics to nanocomposites with uses in the rapidly growing nanotechnology research on synthetic materials (Zhou and Keeling, 2013). For the current study; it was of interest to find out whether the property of plasticity can be reversed by suitable base treatment of the acid washed clays.

METHODOLOGIES

Clay samples used in this work came from a well-known deposit located to the Southeast of Mukurwe-ini sub-County, Nyeri County (Latitude 00°34´00´´S, Longitude 37°03´00´´E), and was collected on site. For each mine, three samples were collected at three depths namely 0.45, 0.9, and 1.5 m. The samples were packed in plastic containers and coded as indicated in the Table 1.

Instrumentation

Atomic absorption and X–ray spectroscopy techniques were used for elemental analysis of the raw and treated clays. Nature of minerals present in raw and treated clays was determined using X-ray diffraction. Calibration of Atomic Absorption Spectrophotometer (AAS) and X-ray fluorescence (XRF) instruments was done using standard rock samples SY-2, MRG-1, and MRG-2procured through Department of Mines and Geology, Ministry of Mining of Kenya.

Sample preparation

Raw clay samples were dried at 105°C in an oven for 6 h, and allowed to cool in desiccators. Samples of the clay so prepared were crushed in a TS 750 Siebtechnik laboratory disc mill to particle size less than 2.00 µm.

Chemical analysis of the clay

Preparation of samples for AAS and XRFS analysis was done using the methods described by Haruna et al. (2007) and Karoki (2009). The raw, acid and base treated samples were subjected to qualitative and quantitative phase analysis, for phase identification and quantification. This was done using a Bruker D2 Phaser. The results were given in form of spectra and the quantities of each mineral present in the sample.

Determination of plasticity index

The constancy limits of the raw and treated clay samples were done using British Standard, 1377: Part 2: 1990).

Treatment of clays with acids

Samples were air-dried and ground to a particle size of 2.00 µm. About 20 g of prepared sample were weighed into a 250 ml Pyrex conical flask and 100 ml of 12 M hydrochloric acid (HCl) added. The resulting slurry was heated at 100°C in a fume chamber, using an electrically heated hot plate for 2 h. Ice-cold distilled water was carefully added to the resulting slurry, which was then filtered using Whatman filter paper No 541 to separate acid matrix from the clay. This filtration was done under gravity. The clay was quenched thoroughly with distilled water. The treatment process was repeated with 10, 8, 6, 4 and 2 M HCl. Treatment was repeated at 200°C. The chemical and mineralogical composition was determined using AAS and XRFS (Onukwuli and Ajemba, 2012). These treatments were repeated with sulphuric (VI), H_2SO_4 acid.

Treatment of acids-treated clays with bases

Approximately 1000 g of dry clay sample was treated with 5000 ml of 12 M hydrochloric acid and heated to 100°C for two hours in a fume chamber. Ice-cold distilled water was added to the mixture, which was then filtered. The residual washed thoroughly with distilled water, dried in an oven at 105°C for 2 h to drive out any moisture present. The dry residue was then divided into 3 portions. A 300 g of the first portion was treated with 600 ml of 0.5 M ammoniumhydroxide (NH_4OH) and allowed to stand for 24 h. The mixture was filtered and residual kept aside for plasticity test and X-ray diffraction analysis. A 300 g of the second portion was treated with same volume of 1.0 M NH_4OH and handled as the first portion. The same amount of the third portion was mixed with 600 ml freshly prepared aluminium hydroxide solution (120.7 g of aluminium chloride hexahydrate ($AlCl_3.6H_2O$) was dissolved in 1000 ml of distilled water and equal volume of 1 M ammonium hydroxide solution added to precipitate the aluminiumhydroxide, $Al(OH)_3$) and given the same treatment as the other portions. Plasticity of the three residues was then determined using the cone penetrometer method. Composition of the base treated clay samples was done using X-ray diffraction analysis (XRD).

RESULTS AND DISCUSSION

Result of elemental analysis of raw clay samples

The results show that Mukurwe-ini clays contain silica and alumina as major quantities; however, MgO, CaO, Na_2O, K_2O, and TiO_2 are present in trace amounts. Iron is also present in the range 1.4 to 4.2% (Table 2). This clay therefore, cannot be used in manufacture of high-grade ceramic products such as white porcelain, glossy paper, and others where clays with less than 1% iron content is required (Karoki, 2009). Furthermore, the SiO_2/Al_2O_3 ratio greater than one is suggestive of a clay suitable not for bleaching but for zeolite development (Usman et. al., 2012).

Analysis using Atterberg limits

The results of determination of Atterberg limits of raw and base-treated samples shows the clays have medium plasticity (Table 3). Comparison of these results with similar work available in literature (Table 4) places Mukurwe-ini clay among kaolinite group but with isomorphic substitution of Al with Na, Mg, K, Ca, and Fe in the clay structure. Using the results of this study, it was interesting to note that the Atterberg limits of the treated clays were highly comparable to those of natural clays(Table 3). This result confirms that the treatment given to the acid washed clays restored the property of plasticity of the treated materials.

XRD analysis of raw Mukurwe-ini clay

Bulk XRD spectrum analysis shows that the raw clay consists of the minerals quartz, albite, microcline, and kaolinite. Phase quantification of the minerals by XRD gave quartz (57.90%), albite (5.30%), microcline (16.10%), and kaolinite (20.80%). The raw clay exhibited well-defined peaks at 2θ values at 12°, 25°, and 38°, which are typical reflections of the clay mineral kaolinite (Panda et al., 2010) and which correspond to d values of 7.17Å and 3.58Å characteristic of the mineral kaolinite (Harris and White, 2007). The spectrum is illustrated in Figure 1.

Analysis of acid washed clays

AAS Analysis of acid washed samples

The results of AAS analysis of the acid washed samples are shown in Tables 5 and 6. It was noted that the chemical composition of the clays changed substantially after acid treatment. Figure 2 provides a summary of changes of iron levels after acid treatment. As the concentration of the acid increased, there was marked increase in dissolution of iron as shown by the its reduced levels compared to the raw (control) sample(Figure 2).

After acid treatment, there was a reduction of Al_2O_3, MgO, CaO, Na_2O, Fe_2O_3, and TiO_2, however K_2O is retained the acid matrix. Acid attack caused fast exchange of hydrated exchangeable cations with H^+, which then attack the structural OH^- groups (Martin et al., 2012). Potassium cations may have reacted with amorphous silica in the matrix to produce potassium feldspar, which is resistant to acid attack (Motlagh et al., 2011). Silica content in the acid washed clays increased. This was caused by leaching of $Al^{3+}$from octahedral layer due acid attack; at higher acid concentrations (above 8 M), there was significant reduction of alumina due severe

Table 2. AAS Elemental analysis of Raw clay samples in percentage of oxides (n=3).

Sample	SiO_2	Al_2O_3	CaO	MgO	Na_2O	K_2O	TiO_2	MnO	Fe_2O_3	LOI	TOT
Muk A1	56.75±0.33	23.04±1.17	0.10±0.01	0.33±0.01	0.27±0.02	1.20±0.06	1.96±0.62	0.01±0.01	1.40±0.12	11.45	96.51
Muk A2	58.04±0.89	22.50±0.34	0.08±0.02	0.35±0.01	0.26±0.04	1.18±0.01	1.78±0.46	0.01±0.01	1.43±0.17	11.47	97.1
Muk A3	82.75±0.94	5.62±0.33	0.08±0.02	0.24±0.06	0.08±0.03	0.40±0.01	0.26±0.08	0.01±0.01	1.86±0.30	6.88	98.18
Muk B1	46.36±0.32	28.38±0.07	0.08±0.03	0.34±0.08	0.11±0.02	0.44±0.02	1.14±0.31	0.01±0.01	2.52±0.12	20.61	99.99
Muk B2	48.31±0.20	27.98±0.28	0.08±0.02	0.34±0.07	0.13±0.02	0.62±0.03	1.12±0.44	0.01±0.01	1.77±0.37	20.26	100.62
Muk B3	54.43±0.58	25.72±0.03	0.10±0.02	0.33±0.06	0.28±0.03	0.97±0.08	1.88±0.17	0.01±0.01	1.70±0.12	15.15	100.57
Muk C1	62.83±1.24	18.72±0.24	0.10±0.01	0.31±0.09	0.31±0.03	0.79±0.03	1.75±0.39	0.01±0.01	1.73±0.17	14.13	100.67
Muk C2	49.75±0.43	24.79±0.35	0.09±0.01	0.29±0.06	0.34±0.07	0.86±0.08	1.24±0.67	0.01±0.01	4.23±0.32	18.17	99.77
Muk C3	77.49±0.59	9.93±0.24	0.10±0.01	0.26±0.08	0.24±0.03	0.96±0.26	0.82±0.26	0.01±0.01	0.96±0.09	8.61	99.38

Table 3. Atterberg limits of raw and treated Mukurwe-ini clay samples.

Sample	Liquid limit (LL) (%)	Plastic limit (PL) (%)	Plasticity index (%)(PI=LL-PL)	Plasticity ratio(R) (R=LL/PL)	Shrinkage limit (%)
Muk A1	65.9	35.2	30.7	1.87	15
Muk A2	65.6	35.2	30.4	1.86	15
Muk A3	66.1	35.9	30.2	1.84	15
Muk B1	44.8	22.5	22.3	1.99	11.4
Muk B2	43.4	20.4	23	2.13	11.4
Muk B3	43.7	20.9	22.8	2.09	11.4
Muk C1	43	18	25	2.39	12.1
Muk C2	43.9	18.9	25	2.32	12.1
Muk C3	42.8	18.4	24.4	2.33	12.1
NH_4OH treated samples	51.0	29.0	22.0	1.76	11.0
$Al(OH)_3$ treated samples	44.9	22.0	22.9	2.04	11.9

leaching of the clay structure leading to de-alumination of the clay (Panda et al., 2010). According to Panda et al. (2010), the reaction between kaolinite and sulphuric acid is described by Equation (1).

$$Al_2O_3 \cdot 2SiO_2 \cdot 2H_2O + 3H_2SO_4 \rightarrow Al_2(SO_4)_3 + 2SiO_2 + 5H_2O \quad (1)$$

Formation of amorphous silica and dissolution of Al^{3+} as in Equation (1) accounts for the increase of silica content and attendant reduction of alumina in the acid treated samples. Loss of ignition of the clays increased after acid treatment. This is due to an increase of amorphous silica that made water adsorption higher (Panda et al., 2010). Clays subjected to acid dissolution at a higher temperature (Table 6) showed high Si/Al ratios, a sign of extensive destruction of the mineral structures caused by discharge of Al^{3+} from octahedral layers (Bowanko and Jozefaciuk, 2002).

XRD analysis of acid washed samples

Analysis of the XRD diffractogram indicates dissolution of the minerals kaolinite and albite in

Table 4. Atterberg limits of some clay minerals (Salvage,2007)

Mineral	Exchangeable ion	Liquid limit (%)	Plastic limit (%)	Plasticity index (%)	Shrinkage limit (%)
Montmorillonite	Na	710	54	656	9.9
	K	660	98	562	9.3
	Ca	510	81	429	10.5
	Mg	410	60	350	14.5
	Fe	290	75	215	10.3
	Fe^{3+}	140	73	67	_
Illite	Na	120	53	67	15.4
	K	120	60	60	17.5
	Ca	100	45	55	16.8
	Mg	95	46	49	14.7
	Fe	110	49	61	15.3
	Fe^{3+}	79	46	33	_
Kaolinite	Na	53	32	21	26.8
	K	49	29	20	_
	Ca	38	27	11	24.5
	Mg	54	31	23	28.7
	Fe	59	37	22	29.2
	Fe^{3+}	56	35	21	_

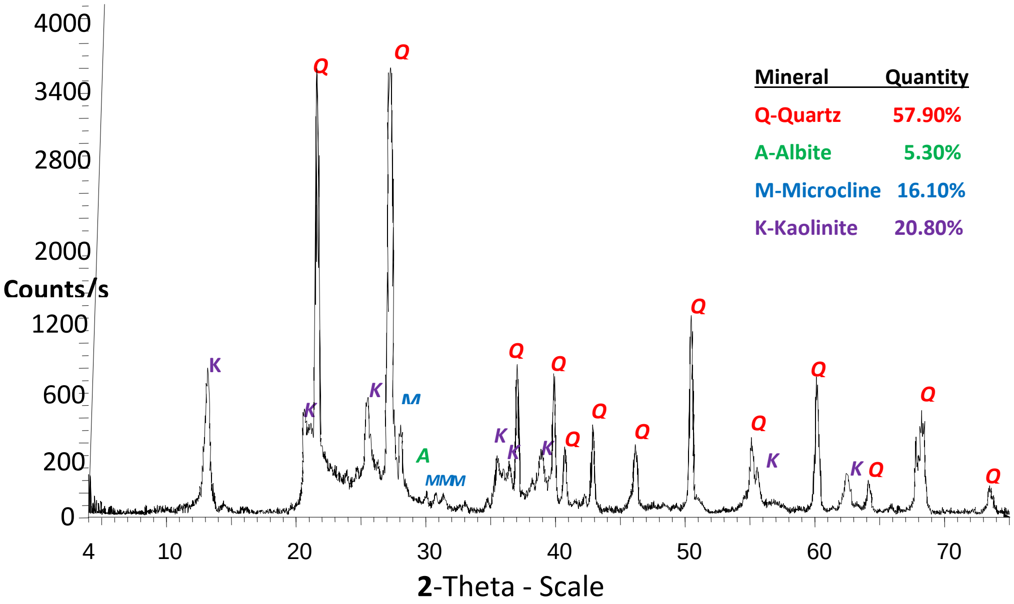

Figure 1. XRD spectrum of raw clay.

the acid, however quartz and microcline are largely unaffected by the acid treatment. Phase quantification after acid treatment was quartz (61.40%), microcline (22.30%), and kaolinite (5.40). Dissolution of the minerals in the acid converted the clay into amorphous silica and as a consequence loss of its plasticity. The retention of the reduced peak means the structure of the clay was only partially affected. The retained peak opened an

Table 5. Summary of treatment of samples with sulphuric acid at 100°C in % oxides composition (n=3).

Concentration	SiO_2 Mean±SE	Al_2O_3 Mean±SE	CaO Mean±SE	MgO Mean±SE	Na_2O Mean±SE	K_2O Mean±SE	TiO_2 Mean±SE	MnO Mean±SE	Fe_2O_3 Mean±SE
Raw sample	59.64±2.37^{a}	20.73±1.48^{c}	0.09±0.00	0.31±0.01^{d}	0.22±0.02	0.82±0.06^{a}	1.34±0.13^{b}	0.01±0.00^{b}	1.95±0.18^{d}
12M	71.46±1.70^{b}	11.78±0.99^{a}	0.08±0.01	0.17±0.01^{b}	0.24±0.02	1.17±0.10^{b}	0.54±0.07^{a}	0.00±0.00^{a}	0.48±0.04^{a}
10M	70.61±1.43^{b}	10.69±0.77^{a}	0.08±0.00	0.17±0.01^{b}	0.24±0.01	1.21±0.11^{b}	0.60±0.06^{a}	0.01±0.00^{b}	0.54±0.03^{a}
8M	67.88±1.40^{b}	13.77±0.84^{ab}	0.08±0.00	0.18±0.01^{b}	0.25±0.01	1.32±0.10^{b}	0.65±0.06^{a}	0.01±0.00^{b}	0.60±0.04^{ab}
6M	65.65±1.29^{b}	15.94±0.88^{b}	0.07±0.00	0.16±0.01^{b}	0.23±0.01	1.10±0.07^{ab}	1.09±0.09^{b}	0.01±0.00^{b}	0.83±0.04^{bc}
4M	58.78±1.34^{a}	16.15±0.73^{b}	0.08±0.00	0.23±0.00^{c}	0.28±0.02	1.10±0.06^{ab}	1.21±0.10^{b}	0.01±0.00^{b}	0.91±0.04^{c}
2M	60.20±2.13^{a}	17.27±1.51^{b}	0.08±0.00	0.11±0.01^{a}	0.26±0.01	1.11±0.07^{ab}	1.11±0.09^{b}	0.01±0.00^{b}	0.92±0.08^{c}
P-value	<0.001	<0.001	0.218	<0.001	0.338	0.002	<0.001	<0.001	<0.001

Mean values within the same column followed by different small letter(s) do not differ significantly (one-way ANOVA, SNK-test=0.05).

Table 6. Summary of treatment of samples with Sulphuric Acid at 200°C in % Oxides composition (n=3).

Concentration	SiO_2Mean±SE	Al_2O_3 Mean±SE	CaO Mean±SE	MgO Mean±SE	Na_2O Mean±SE	K_2O Mean±SE	TiO_2 Mean±SE	MnO Mean±SE	Fe_2O_3 Mean±SE
Raw sample	59.64±2.34^{a}	20.73±1.48^{d}	0.09±0.00^{b}	0.31±0.01^{b}	0.22±0.02^{b}	0.82±0.06	1.34±0.13^{d}	0.01±0.00^{c}	1.95±0.18^{d}
10M	79.88±1.47^{c}	3.30±0.30^{a}	0.09±0.01^{b}	0.20±0.00^{b}	0.18±0.01^{a}	0.78±0.07	0.46±0.06^{a}	0.00±0.00^{a}	0.11±0.01^{a}
8M	77.64±1.68^{c}	8.83±0.88^{b}	0.08±0.00^{b}	0.30±0.07^{b}	0.18±0.01^{a}	0.80±0.08	0.78±0.09^{b}c	0.01±0.00^{c}	0.32±0.03^{ab}
6M	74.81±1.82^{c}	9.69±1.10^{b}	0.06±0.00^{a}	0.12±0.02^{b}	0.16±0.01^{a}	3.58±2.79	0.96±0.09^{c}	0.01±0.00^{c}	0.37±0.05^{ab}
4M	75.91±1.56^{c}	10.00±0.86^{b}	0.06±0.00^{a}	0.23±0.00^{b}	0.17±0.01^{a}	0.72±0.06	0.63±0.06^{ab}	0.01±0.00^{c}	0.44±0.03^{b}
2M	67.32±2.39^{b}	17.28±1.41^{c}	0.07±0.01^{a}	0.28±0.01^{b}	0.16±0.01^{a}	0.68±0.06	0.83±0.07^{bc}	0.02±0.00^{d}	0.82±0.07^{c}
P-value	<0.001	<0.001	<0.001	<0.001	0.007	0.405	<0.001	<0.001	<0.001

opportunity of restoring back the lost properties of the acid washed clays (Figure 3). The preserved peak opened an opportunity of restoring back the lost properties of the acid washed clays. The spectra is shown in Figure 3.

XRD results of base treated acid-activated clays

The result of analysis of base treated acid-activated showed restoration of kaolinite reflections at its typical 2Ө values, though with a slightly reduced intensity. The acid-activated clay treated with ammonium hydroxide had the following phase quantities; quartz (61.70%), microcline (22.30%), and kaolinite (16.30%). The protonated amorphous silica phase reacted with hydroxyl ions of the base to form the mineral kaolinite, hence increase of kaolinite from 5.40% in the acid washed clay to 16.30% in the base acid-activated material (this can be explained by Equation (2)). The diffractograms for acid washed material subjected to ammonium hydroxide and aluminium hydroxide treatment are shown in Figures 4 and 5 respectively.

$$4H^{+} + SiO_2 + 2KAlSi_3O_8 + 2(OH)^{-} \rightarrow Al_2Si_2O_5(OH)_4 + 2K^{+} + 5SiO_2 + H_2O \qquad (2)$$

The XRD spectra of raw and phase quantification of raw and base acid-activated materials are comparable in many ways, an indication of reversal of physico-chemical properties of the acid-washed samples by exposure to the chosen bases. This fact was further reinforced by

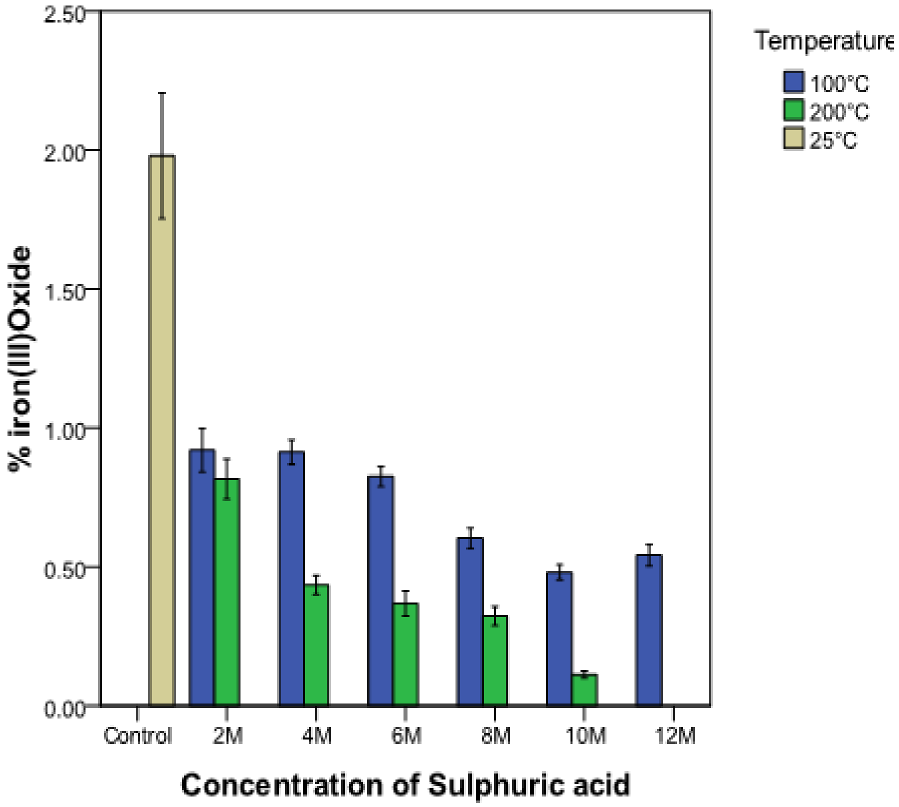

Figure 2. Comparison of Iron Removal by Sulphuric (VI) Acid at 100ºC and 200ºC using sample Muk B2.

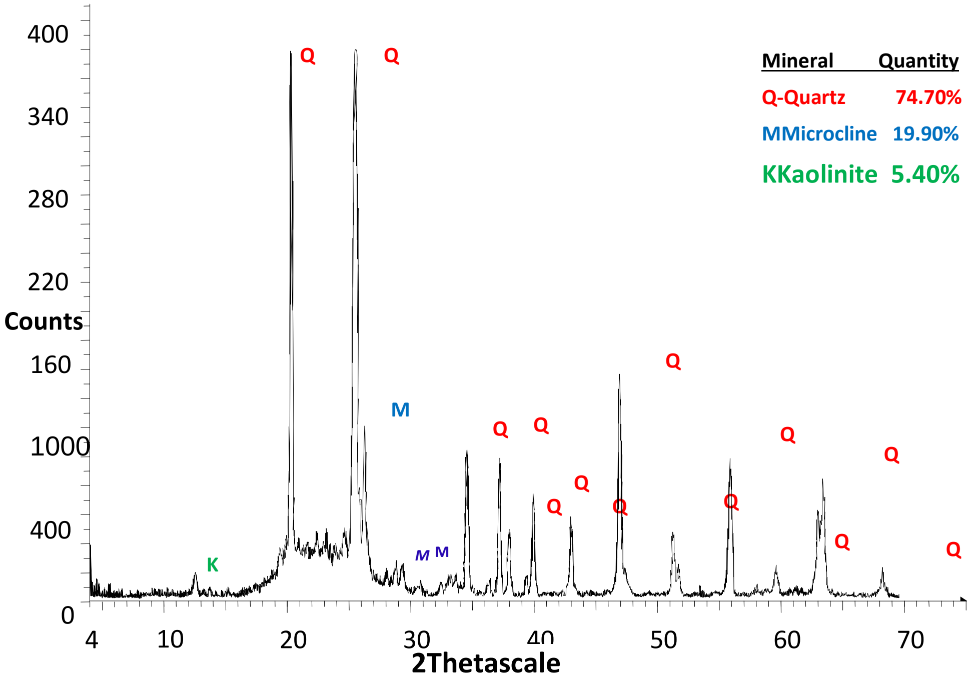

Figure 3. XRD spectra of acid washed clay.

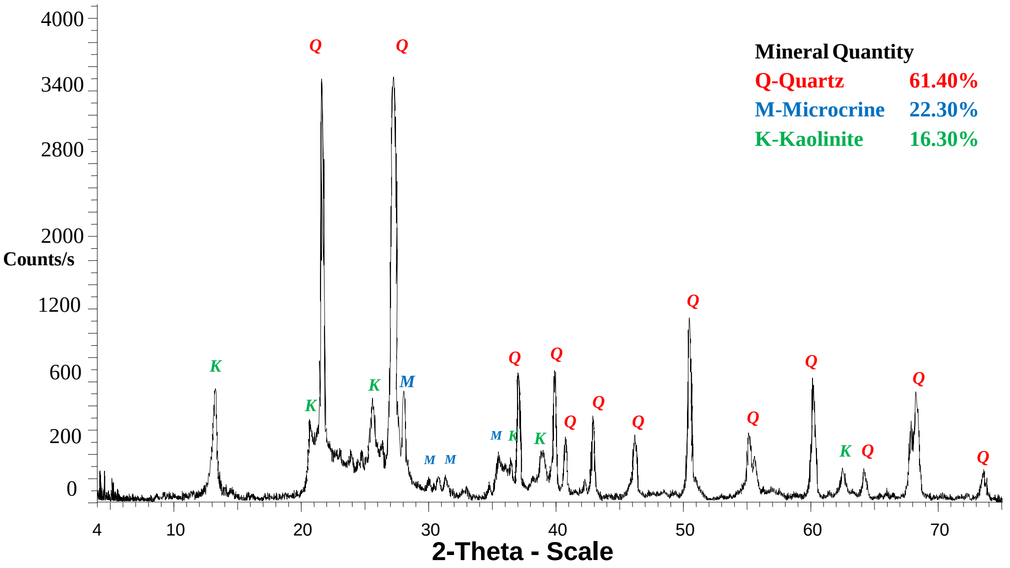

Figure 4. XRD spectra of acid-activated clay treated with dilute ammonium hydroxide.

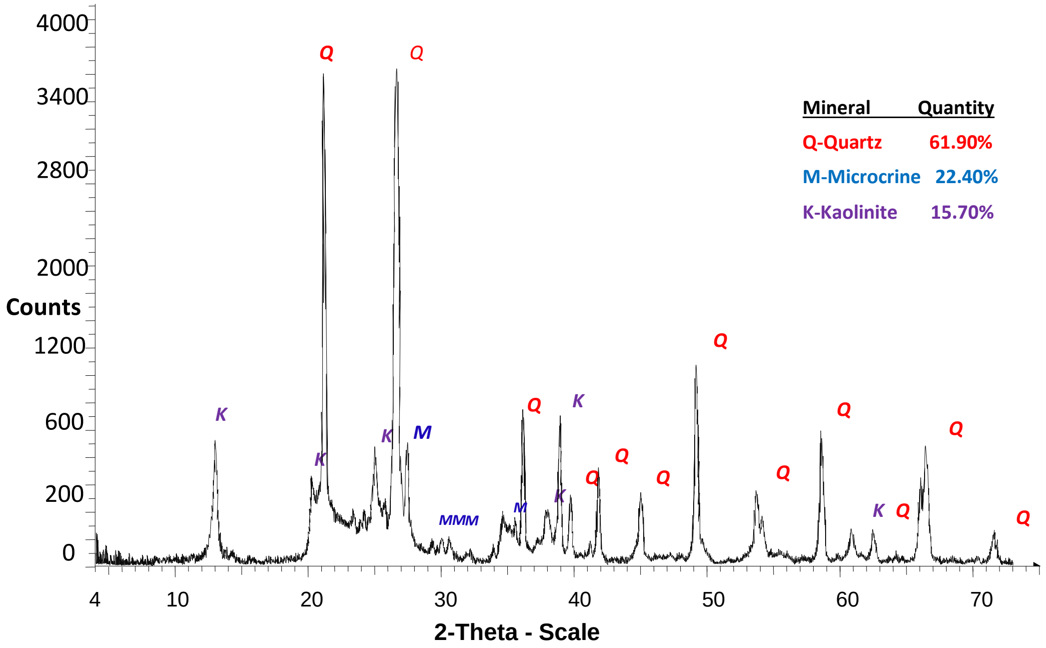

Figure 5. XRD spectra of sample treated with aluminium hydroxide.

comparison of the Atterberg limits of the raw and treated materials, which bear very strong similarities (Table 3).

Conclusion

This study has established that the major minerals in Mukurwe-ini clay include quartz (57.69%), kaolinite (20.80%), albite (5.30%), and microcline (16.10%), evidently kaolinite is the only clay mineral present in this clay. From the XRD analysis of the clay, sodium and potassium are retained in the clay as the minerals albite ($NaAlSi_3O_8$) and microcline ($KAlSi_3O_8$) respectively, commonly called the feldspars. Presence of Kaolinite mineral in the clay makes it suitable for use in ceramics. This study has also shown that the quality of the clay is noticeably improved by acid treatment by reducing its iron content to less than 1%, which is ideal for making high-grade ceramics or in other specialized applications such as in paper industry, catalysis, filler material, white cement and many others where clay purity is required. As the only clay mineral present, kaolinite imparted plasticity on the clay, plasticity index was found to range between 22.3 to 30.7% for the raw samples. The base treated acid-activated material had a PI value of 22.0, which is comparable to those of raw samples a clear reversal of plasticity lost during acid thermal treatment. High levels of silica (57.90%) and feldspars (21.40%) means the geological processes of clay minerals formation is still ongoing in the study area, furthermore this is a sign of geologically young residual clays.

Conflict of Interest

The authors have not declared any conflict of interest.

REFERENCES

Andrade A, Dachamir H, Hazim A (2010). Measuring and modeling plasticity of clay. Mater. Res. 13(3*)*:395-399.

Atkins P, Overton T, Rourke J, Weller M, Armstrong F (2006). Shriver & Atkins Inorganic Chemistry (Fourth Edition). New York: Oxford University Press pp. 168, 338, 628.

Bain A (1971). A plasticity Chart as an aid to the identification and assessment of industrial Clays. Clay and Clay minerals. 9(1):1-17.

Bowanko G, Jozefaciuk G (2012). Effect of acid and alkali treatments on surface areas and adsorption energies f selected minerals. clay and clay minerals. *50*(6):771-783.

British Standard 1377: Part 2 1990. “Soil testing Mechanics,” Laboratory Testing Manual 2000, Central Materials Laboratory, Ministry of Works, The United Republic of Tanzania.

Cao W, Liao L, Zhohui S, Wang X, Zhiguo X (2011). Adsorption of low concentration Ammonium onto Vermiculite from Hebei Province, China. Clay and Clay Minerals 59*(*4):446-458.

Dumbleton MJ, West G (1966). Some factors affecting the relation between the clay minerals in soils and their plasticity. Clay and clay Minerals 6*:*179-193.

Grim E (1979). Clay uses. In Kirk, E. and Othmer, F. (Ed.), *Encyclopedia of Chemical Technology* (Third Edition., New York: John Wiley and Sons 6:207-223.

Gulgun Y (2011). The effect of temperature on characteristics of Kaolin and Bentonite. Sci. Res. Essays *6*(9):1928-1939.

Harris W, White N (2007). Methods of soil analysis. Part 5. Mineralogical methods. SSSA Book Series No.5, Soil Society of America, Madison, USA. 4:36.

Haruna K, Onoja P, Chiroma M (2007). Characterization of Mayo-Belwa clays. Leonardo Electronic J. Practices Technol. *6*(11):123-130.

Igbokwe K, Olebunne L, Nwakandu S (2011). Effect of Activation Parameters on conversion In Clay-Catalyzed Esterification of Acetic acid. Int. J. Basic appl. Sci. (IJBAS-IJENS) 11(5):1-8.

Julia NR, Lawrence NW (2011). Hydration behaviour of MX80.bentonite in a confined volume system: Implications for backfill design. Clay and Clay Minerals *59*(4):640-653.

Karoki K (2009). Analysis and treatment of clays from Mwea to assess their value as a source of Aluminium and Ceramic products. (Master of Science Un-Published), Kenyatta, Nairobi, Kenya. pp. 3-31.

Keller D (1979). Clays. In Kirk, E. and Othmer, F. (Ed), Encyclopedia of Chemical Technology (Third Edition). New York. John Wiley and Sons 6:190-206.

Mohamed AA, Hesham GI (2010). Variation of Feed Chemical Composition and Its Effect on Clinker Formation–Simulation Process. Proceedings of the World Congress on Engineering and Computer Science 2010 Vol II WCECS 2010, October 20-22, 2010, San Francisco, USA.

Motlagh KM, Youzbashi AA, Rigi AZ (2011). Effect of acid activation on structural and bleaching properties of a Bentonite*.* Iranian J. Mat. Sci. Eng. 9(4):50–56.

Neville AM (2012). Properties of Concrete (Fifth Edition), London, Prentice Hall Chapter 1 Safaribooksonline.com Web ISBN-10:0-273-78633-78634.

Onukwuli D, Ajemba R (2012). Evaluation of the Effects of acid activation on adsorptive properties of Clay from Ukpor in bleaching Palm oil. Int. J. Multidisciplinary Sci. *3*(5):46-52.

Panda AK, Mishra BG, Mishra DK, Singh RK (2010). Effect of sulphuric acid treatment on the physic-chemical characteristics of kaolin clay. Colloid and surfaces A: Physiochemical and Engineering Aspects 363(2010):98-104.

Salvage PF (2007). Evaluation of possible swelling potential of soils. Proceedings of the 26th Southern African Transport Conference (SATC, 2007). Pretoria, South Africa pages 277 – 282 ISBN 1-920-01702-x. 9-12 July 2007 online at repository.up.ac.za/bitstream/handle/2263/5947/040.pdf. Accessed 20/6/2013.

Schoonheydt R, Johnson T (2006). Surface and Interface Chemistry of Clay Minerals .In Lagaly, G., Theng, K., Bergaya, F., (Ed.) Handbook of Clay Science. Development in Clay Science (Vol.1). Amsterdam: Elsevier Ltd. Chapter 3.

Stucki W (2006). Properties of iron in clays. In Lagaly, G., Theng, K., Bergaya. F, (Ed.) Handbook of Clay Science. Development in Clay Science (Vol.1) AMSTERDAM, Elsevier Ltd. P.424.

Stucki W, Golden C, Charles R (1984a). Effects of reduction and re-oxidation of structural iron on the surface charge dissolution of Smectites. Clay and Clay minerals. *32*(5):350-356.

Stucki W, Golden C, Charles R, Philip L (1984b). Effects of oxidation state of octahedral iron on Clay swelling. Clay and Clay Minerals *32*(5):357-362.

Usman MA, Ekwueme KI, Alaje TO, Mohammed AO (2012). Research article, Characterization, acid activation, and bleaching performance of Ibeshe clay, Lagos, Nigeria. International Scholarly Research Network volume 2012, *Article ID 658508,5 pages.* Doi:10.5402/2012/658508. Accepted 11 January, 2012.

Vaughan J, Patrick D (1995). The Mineralogy Society Series. Mineral Surfaces. London: Chapman Hall. pp. 303-323.

Yahiaoui A, Mohammed B, Hachemaoui A (2003). An Acid Exchanged Montmorillonite Clay-Catalyzed Synthesis of Polyepichlorhydrin. Int. J. Mol. Sci*.* 4:548-561.

Zhou C, Keeling J (2013). Fundamental and applied research on clay minerals: From climate and environment to nanotechnology. Appl. clay sci. 74:3-9.

African Journal of Pure and Applied Chemistry